Columbia University
in the City of New York

DEPARTMENT OF CIVIL ENGINEERING

FURTHER STUDIES OF THE RESPONSE OF A CYLINDRICAL SHELL TO A TRANSVERSE SHOCK WAVE

by

M. L. BARON and H. H. BLEICH

Office of Naval Research
Contract Nonr-266(08)
Technical Report No. 10
CU-10-53-ONR-266(08)-C.E.
December 1953

Columbia University
in the City of New York

DEPARTMENT OF CIVIL ENGINEERING

FURTHER STUDIES OF THE RESPONSE OF A CYLINDRICAL SHELL TO A TRANSVERSE SHOCK WAVE

by

M. L. BARON and H. H. BLEICH

Office of Naval Research
Contract Nonr-266(08)
Technical Report No. 10
CU-10-53-ONR-266(08)-C.E.
December 1953

TABLE OF CONTENTS

		Page
List of Symbols		iii
I	Introduction	v
II	Interaction between Shell and Medium	1
III	Response of Shell to a Step Shock Wave for $n \geq 1$	3
IV	Accuracy of the Approximation, Eq. (II-20)	9
V	Comparison of Results of Extensional and Inextensional theories	9
	a) Buoyant Shell, $\frac{\rho a}{2m} = 1$, $n = 1$	9
	b) Light Shell, $\frac{\rho a}{2m} = 5$, $n = 1$	9
	c) Light Shell, $\frac{\rho a}{2m} = 5$, $n = 2$	9
VI	Shell with an Additional Mass	11
VII	Summation of Effects from all Modes, Pressure of Medium	12
VIII	Total Acceleration, Stress and Fluid Pressure for Small Values of t	13
References		17
Appendix		19
Fig. 1-23		

LIST OF SYMBOLS[1]

θ,r	Polar coordinates, See Fig. 1.
w, v	Radial and tangential displacements of the cylindrical shell. Note that a positive displacement w is inward.
A	Cross sectional area of the cylindrical shell.
a	Radius of the cylinder.
c	Velocity of sound in medium.
c_s	Velocity of sound in shell.
d	Distance from neutral axis of the shell to the extreme fiber.
d_n	Coefficient defining the shape of the modes in vacuo.
C_k, z_k, μ_k	See Eq. (III-4) – (III-6).
E	Modulus of Elasticity.
h	Thickness of shell.
$H_n^{(2)}$	Hankel function of second kind of order n.
I_n	Modified Bessel function of the first kind of order n.
K	Spring constant per unit area of shell (Section VIII)
m	Mass of shell per unit area.
$m_n, \bar{m}_n$	Generalized masses.
M	Additional mass per unit length of shell (Section VIII).
n	Number of circumferential waves of mode.
$p(\theta, t)$	Shock wave pressure on surface of the shell.
p	Constant peak pressure of shock wave.
$P_n(t)$	t dependent expansion coefficient of $p(\theta,t)$.
$P_n^{(t)}$	t dependent expansion coefficient of $Z(\theta,t)$.
$q_n, \bar{q}_n$	Generalized coordinates.
T	Kinetic Energy.
t	Time.
$v(\theta,t)$	Radial component of particle velocity of the shock wave.
$V_n(t)$	t dependent expansion coefficient of $v(\theta,t)$.
x	Displacement of the added mass M.
X_n	Coefficient, $x = X_n q_n e^{i\Omega t}$
$Z(\theta,t)$	Fluid pressure on the surface of the shell.
$\alpha = \cos^{-1}(1 - \frac{ct}{a})$	Angle of envelopment
$\delta, \bar{\delta}$	See Eq. (III-1).
ϵ	Hoop strain.

(1) Additional symbols in the appendix are defined as they occur.

I Introduction

The response of an elastic cylindrical shell to a transverse shock wave was obtained by Mindlin and Bleich (1) by an expansion of the response into normal modes of oscillation, neglecting extensional effects, except in the dilational mode, n = O. An alternative solution of the problem by Carrier (2) also neglects these extensional effects. The first part of the present paper, Sections II – V, is devoted to the presentation of a refined method allowing for the extensional effects in all modes. Although these effects damp out ultimately, they are necessarily of importance very shortly after the arrival of the shock wave. While the largest stresses in the shell occur at late stages when the shell is fully enveloped, shock effects develop much earlier and the refined theory is of importance for their study.

Except for the inclusion of extensional effects the basic assumptions and method of approach are identical with those of reference 1. The cylindrical shell is elastic, circular in cross-section, homogeneous and infinitely long. It is submerged in an acoustic medium, i.e. one whose motions conform to the linear theory of waves of expansion. The shell is subjected to a plane shock wave, with its wave front parallel to the axis of the cylinder. By means of an approximation, the potential of the diffraction and radiation is eliminated between the simultaneous equations which couple the generalized coordinates of the shell and the fluid. As a result, pairs of second order linear simultaneous differential equations are obtained, linking the essentially inextensional bending modes of the shell with the essentially extensional modes.

The solution of this system of simultaneous differential equations is reduced in general to a sum of four definite integrals during the time of transit of the shock wave across the shell, and for a step shock wave, it can be expressed in terms of tabulated functions thereafter.

The differences in the results of the present paper and of the method of ref. 1 are evaluated for typical cases.

Section VI contains a different generalization of the problem treated in ref. 1. It considers the case of an inextensional shell which encloses and supports an additional concentrated mass on the centerline of the shell.

The final sections VII and VIII are devoted to a consideration of the total effects from all generalized coordinates (modes) of differing n. It is shown how quite simple approximate solutions for the total effects can be obtained for the early stages of the interaction problem. It is found that these solutions are upper limits for the correct ones. It is concluded that these early time solutions are significant for accelerations and shock effects, while the stresses due to shock waves of long duration can be determined by the mode approach.

II) Interaction between Shell and Medium.

The response of an elastic cylindrical shell to a transverse shock wave is studied in this paper by considering the shell without the fluid as a separate structure responding to the dynamic forces exerted by the surrounding infinite acoustic medium. Using the modes of free vibration of the shell in vacuo as generalized coordinates, its response can be expressed in terms of the infinite number of these modes.

The shock wave is assumed to be plane, with its wave front parallel to the axis of the shell. Such a wave will only excite those modes of the shell in which the generators of the cylinder remain straight, and the frequencies and modes required are those of a thin circular ring determined in the Appendix. The individual modes can be classified by the integral number n of circumferential waves. For each number $n > 0$ there exist two frequencies, one corresponding to a primarily inextensional (bending) mode and the other to a primarily extensional mode. The displacements w and v, Fig. 1, of the former are given by:

$$\begin{aligned} w &= \cos n\theta \\ v &= \frac{1}{d_n} \sin n\theta \end{aligned} \qquad (n \neq 0) \tag{II-1}$$

while those of the latter are given by:

$$\begin{aligned} w &= \cos n\theta \\ v &= -d_n \sin n\theta \end{aligned} \qquad (n = 0, 1, 2, ..) \tag{II-2}$$

The displacement of the shell may now be expressed by generalized coordinates $\bar{q}_o$, q_n and $\bar{q}_n$ $(n \neq 0)$:

$$w(\theta,t) = \bar{q}_o + \sum_{n=1}^{\infty} (q_n + \bar{q}_n) \cos n\theta \tag{II-3}$$

$$v(\theta,t) = \sum_{n=1}^{\infty} \left(\frac{q_n}{d_n} - d_n \bar{q}_n\right) \sin n\theta \tag{II-4}$$

The fluid pressure Z acting on the surface of the cylinder is expanded:

$$Z = \sum_{n=0}^{\infty} Q_n(t) \cos n\theta . \tag{II-5}$$

The equations of cylindrical motion of the shell may be written in terms of the generalized coordinates q_n and $\bar{q}_n$.

$$\ddot{q}_n + \omega_n^2 q_n = \frac{Q_n}{m_n} \qquad n = 1, 2, 3 .. \tag{II-6}$$

$$\ddot{\bar{q}}_n + \bar{\omega}_n^2 \bar{q}_n = \frac{Q_n}{\bar{m}_n} \qquad n = 0, 1, 2, 3 .. \tag{II-7}$$

where

$$m_n = m\left(1 + \frac{1}{d_n^2}\right) \tag{II-8}$$

$$\bar{m}_n = m(1 + d_n^2) \tag{II-9}$$

TABLE OF CONTENTS

		Page
List of Symbols		iii
I	Introduction	v
II	Interaction between Shell and Medium	1
III	Response of Shell to a Step Shock Wave for $n \geq 1$	3
IV	Accuracy of the Approximation, Eq. (II-20)	9
V	Comparison of Results of Extensional and Inextensional theories	9
	a) Buoyant Shell, $\frac{\rho a}{2m} = 1$, $n = 1$	9
	b) Light Shell, $\frac{\rho a}{2m} = 5$, $n = 1$	9
	c) Light Shell, $\frac{\rho a}{2m} = 5$, $n = 2$	9
VI	Shell with an Additional Mass	11
VII	Summation of Effects from all Modes, Pressure of Medium	12
VIII	Total Acceleration, Stress and Fluid Pressure for Small Values of t	13
References		17
Appendix		19
Fig. 1-23		

LIST OF SYMBOLS[1]

θ,r	Polar coordinates, See Fig. 1.
w, v	Radial and tangential displacements of the cylindrical shell. Note that a positive displacement w is inward.
A	Cross sectional area of the cylindrical shell.
a	Radius of the cylinder.
c	Velocity of sound in medium.
c_s	Velocity of sound in shell.
d	Distance from neutral axis of the shell to the extreme fiber.
d_n	Coefficient defining the shape of the modes in vacuo.
C_k, z_k, μ_k	See Eq. (III-4) – (III-6).
E	Modulus of Elasticity.
h	Thickness of shell.
$H_n^{(2)}$	Hankel function of second kind of order n.
I_n	Modified Bessel function of the first kind of order n.
K	Spring constant per unit area of shell (Section VIII)
m	Mass of shell per unit area.
$m_n, \bar{m}_n$	Generalized masses.
M	Additional mass per unit length of shell (Section VIII).
n	Number of circumferential waves of mode.
$p(\theta, t)$	Shock wave pressure on surface of the shell.
p	Constant peak pressure of shock wave.
$P_n(t)$	t dependent expansion coefficient of $p(\theta,t)$.
$P_n^{(t)}$	t dependent expansion coefficient of $Z(\theta,t)$.
$q_n, \bar{q}_n$	Generalized coordinates.
T	Kinetic Energy.
t	Time.
$v(\theta,t)$	Radial component of particle velocity of the shock wave.
$V_n(t)$	t dependent expansion coefficient of $v(\theta,t)$.
x	Displacement of the added mass M.
X_n	Coefficient, $x = X_n q_n e^{i\Omega t}$
$Z(\theta,t)$	Fluid pressure on the surface of the shell.
$\alpha = \cos^{-1}(1 - \frac{ct}{a})$	Angle of envelopment
$\delta, \bar{\delta}$	See Eq. (III-1).
ϵ	Hoop strain.

---

(1) Additional symbols in the appendix are defined as they occur.

I Introduction

The response of an elastic cylindrical shell to a transverse shock wave was obtained by Mindlin and Bleich (1) by an expansion of the response into normal modes of oscillation, neglecting extensional effects, except in the dilational mode, n = O. An alternative solution of the problem by Carrier (2) also neglects these extensional effects. The first part of the present paper, Sections II – V, is devoted to the presentation of a refined method allowing for the extensional effects in all modes. Although these effects damp out ultimately, they are necessarily of importance very shortly after the arrival of the shock wave. While the largest stresses in the shell occur at late stages when the shell is fully enveloped, shock effects develop much earlier and the refined theory is of importance for their study.

Except for the inclusion of extensional effects the basic assumptions and method of approach are identical with those of reference 1. The cylindrical shell is elastic, circular in cross-section, homogeneous and infinitely long. It is submerged in an acoustic medium, i.e. one whose motions conform to the linear theory of waves of expansion. The shell is subjected to a plane shock wave, with its wave front parallel to the axis of the cylinder. By means of an approximation, the potential of the diffraction and radiation is eliminated between the simultaneous equations which couple the generalized coordinates of the shell and the fluid. As a result, pairs of second order linear simultaneous differential equations are obtained, linking the essentially inextensional bending modes of the shell with the essentially extensional modes.

The solution of this system of simultaneous differential equations is reduced in general to a sum of four definite integrals during the time of transit of the shock wave across the shell, and for a step shock wave, it can be expressed in terms of tabulated functions thereafter.

The differences in the results of the present paper and of the method of ref. 1 are evaluated for typical cases.

Section VI contains a different generalization of the problem treated in ref. 1. It considers the case of an inextensional shell which encloses and supports an additional concentrated mass on the centerline of the shell.

The final sections VII and VIII are devoted to a consideration of the total effects from all generalized coordinates (modes) of differing n. It is shown how quite simple approximate solutions for the total effects can be obtained for the early stages of the interaction problem. It is found that these solutions are upper limits for the correct ones. It is concluded that these early time solutions are significant for accelerations and shock effects, while the stresses due to shock waves of long duration can be determined by the mode approach.

II) Interaction between Shell and Medium.

The response of an elastic cylindrical shell to a transverse shock wave is studied in this paper by considering the shell without the fluid as a separate structure responding to the dynamic forces exerted by the surrounding infinite acoustic medium. Using the modes of free vibration of the shell in vacuo as generalized coordinates, its response can be expressed in terms of the infinite number of these modes.

The shock wave is assumed to be plane, with its wave front parallel to the axis of the shell. Such a wave will only excite those modes of the shell in which the generators of the cylinder remain straight, and the frequencies and modes required are those of a thin circular ring determined in the Appendix. The individual modes can be classified by the integral number n of circumferential waves. For each number $n > 0$ there exist two frequencies, one corresponding to a primarily inextensional (bending) mode and the other to a primarily extensional mode. The displacements w and v, Fig. 1, of the former are given by:

$$\begin{aligned} w &= \cos n\,\theta \\ v &= \frac{1}{d_n} \sin n\,\theta \end{aligned} \qquad (n \neq 0) \qquad \text{(II-1)}$$

while those of the latter are given by:

$$\begin{aligned} w &= \cos n\,\theta \\ v &= -d_n \sin n\,\theta \end{aligned} \qquad (n = 0, 1, 2, ..) \qquad \text{(II-2)}$$

The displacement of the shell may now be expressed by generalized coordinates $\bar{q}_o$, q_n and $\bar{q}_n$ $(n \neq 0)$:

$$w(\theta,t) = \bar{q}_o + \sum_{n=1}^{\infty} (q_n + \bar{q}_n) \cos n\,\theta \qquad \text{(II-3)}$$

$$v(\theta,t) = \sum_{n=1}^{\infty} \left(\frac{q_n}{d_n} - d_n\,\bar{q}_n\right) \sin n\,\theta \qquad \text{(II-4)}$$

The fluid pressure Z acting on the surface of the cylinder is expanded:

$$Z = \sum_{n=0}^{\infty} Q_n(t) \cos n\,\theta\,. \qquad \text{(II-5)}$$

The equations of cylindrical motion of the shell may be written in terms of the generalized coordinates q_n and $\bar{q}_n$.

$$\ddot{q}_n + \omega_n^2 q_n = \frac{Q_n}{m_n} \qquad n = 1, 2, 3 .. \qquad \text{(II-6)}$$

$$\ddot{\bar{q}}_n + \bar{\omega}_n^2 \bar{q}_n = \frac{Q_n}{\bar{m}_n} \qquad n = 0, 1, 2, 3 .. \qquad \text{(II-7)}$$

where

$$m_n = m\left(1 + \frac{1}{d_n^2}\right) \qquad \text{(II-8)}$$

$$\bar{m}_n = m(1 + d_n^2) \qquad \text{(II-9)}$$

ω_n^2 and $\bar{\omega}_n^2$ are the natural frequencies of the vibrations of the shell in vacuo, corresponding to the displacements of Eq. (II-1) and (II-2) respectively. The values of these frequencies are given in the Appendix, Eq. (A-8).

The coefficient d_n depends on the ratio of the bending to the extensional stiffness. For cases of practical interest, and for the lower modes ($n \leq 5$), there is practically no coupling between the bending and extensional effects and the value of d_n is very close to $d_n = n$. In such cases, simplified expressions are obtained for m_n, $\bar{m}_n$, ω_n and $\bar{\omega}_n$. (See Appendix, Eqs. A-12,13,23).

Proceeding exactly as in ref. 1, the pressure on the shell is considered due to the shock wave, and due to the waves reflected and radiated from the vibrating shell:

$$Z = p(\theta,t) + \rho \dot{\phi}\,(a, \theta,t) \tag{II-10}$$

The velocity potential ϕ of the reflected and radiated waves is governed by the equation:

$$c^2 \nabla^2 \phi = \ddot{\phi} \tag{II-11}$$

where c is the velocity of sound in the fluid. With

$$p\,(\theta,t) = \sum_{n=0}^{\infty} P_n(t) \cos n\,\theta \tag{II-12}$$

$$\phi\ (r, \theta, t) = \sum_{n=0}^{\infty} \psi_n(r,t) \cos n\,\theta \tag{II-13}$$

Eq. (II-10) yields the relation

$$Q_n\ (t) = P_n\ (t) + \rho\ \dot{\psi}_n\ (a,t) \tag{II-14}$$

and Eqs. (II-6) and (II-7) become, on r = a

$$\ddot{q}_n + \omega_n^2\, q_n = \frac{(P_n + \rho\ \dot{\psi}_n)}{m_n} \tag{II-15}$$

$$\ddot{\bar{q}}_n + \bar{\omega}_n^2\, \bar{q}_n = \frac{(P_n + \rho\ \dot{\psi}_n)}{\bar{m}_n} \tag{II-16}$$

The radial velocity of a point on the shell must equal the sum of the radial components of the particle velocities of the shock wave and the diffracted wave. Hence:

$$\dot{w} = v\,(\theta,t) + \frac{\partial\, \phi_n\,(a,\theta,t)}{\partial\, a} \tag{II-17}$$

Letting

$$v(\theta,t) = \frac{1}{\rho c} \sum_{n=0}^{\infty} V_n\,(t) \cos n\,\theta \tag{II-18}$$

then, on r = a

$$(\dot{q}_n + \dot{\bar{q}}_n) = \frac{V_n}{\rho c} + \frac{\partial\, \psi_n\,(a,t)}{\partial a} \tag{II-19}$$

The potential function ψ_n can be eliminated by using the approximate expression:

$$\frac{\partial \psi_n (a,t)}{\partial a} = -\frac{1}{c} \frac{\partial \psi_n (a,t)}{\partial t} \qquad (II\text{-}20)$$

derived in ref. 1. The main effect of the approximation is to give the reflection and radiation, associated with each mode of the shell, the propagation characteristics of plane waves rather than cylindrical waves.

Using Eqs. (II-14), (II-19) and (II-20), the relation

$$Q_n(t) = P_n(t) + V_n(t) - \rho c (\dot{q}_n + \dot{\bar{q}}_n) \qquad (II\text{-}21)$$

is obtained and Eqs. (II-15) and (II-16) become:

$$\ddot{q}_n + \frac{\rho c}{m_n} (\dot{q}_n + \dot{\bar{q}}_n) + \omega_n^2 q_n = \frac{P_n + V_n}{m_n} = \frac{S_n}{m_n} \qquad (II\text{-}22)$$

$$\ddot{\bar{q}}_n + \frac{\rho c}{\bar{m}_n} (\dot{q}_n + \dot{\bar{q}}_n) + \bar{\omega}_n^2 \bar{q}_n = \frac{P_n + V_n}{\bar{m}_n} = \frac{S_n}{\bar{m}_n} \qquad (II\text{-}23)$$

The response of the shell to a quite general shock wave is obtained by integrating the set of simultaneous second order linear differential equations with the appropriate $S_n = P_n + V_n$. The fluid pressure is then obtained from Eq. (II-21). For the case of a step shock wave, the values of P_n and V_n are given in reference 1.

III) Response of Shell to a Step Shock Wave for $n \geq 1$.

For the case $n = 0$, only one equation is obtained which is identical with the one obtained in reference I. This case is therefore not considered further.

For $n \geq 1$, Eqs. (II-22, II-23) are integrated by the method of variation of constants. In the following equations the subscripts n are omitted for simplicity, except in the terms m_n and $\bar{m}_n$. With,

$$\delta = \frac{\rho c}{m_n} \quad , \quad \bar{\delta} = \frac{\rho c}{\bar{m}_n} \qquad (III\text{-}1)$$

Eqs. (II-22, II-23) become:

$$\ddot{q} + \delta (\dot{q} + \dot{\bar{q}}) + \omega^2 q = \frac{S}{m_n} \qquad (III\text{-}2)$$

$$\ddot{\bar{q}} + \bar{\delta} (\dot{q} + \dot{\bar{q}}) + \bar{\omega}^2 \bar{q} = \frac{S}{\bar{m}_n} \qquad (III\text{-}3)$$

Let

$$q = \sum_{k=1}^{4} C_k e^{-z_k t}$$

$$\bar{q} = \sum_{k=1}^{4} C_k \mu_k e^{-z_k t} \qquad (III\text{-}4)$$

Substitution into the homogeneous form of Eqs. (III-2, III-3) yields the characteristic equation,

$$z^4 - (\delta + \bar{\delta})\, z^3 + (\omega^2 + \bar{\omega}^2)\, z^2 - (\delta \bar{\omega}^2 + \bar{\delta}\, \omega^2)\, z + (\omega^2\, \bar{\omega}^2) \;=\; 0 \tag{III-5}$$

and the value of μ_k ,

$$\mu_k \;=\; \frac{z_k^2 \;-\; \delta z_k \;+\; \omega^2}{\delta z_k} \tag{III-6}$$

Hence, using Eqs. (III-5) and (III-6), Eqs. (III-4) become:

$$\begin{aligned} q \;&=\; \sum_{k=1}^{4} C_k e^{\,-z_k t} \\ \bar{q} \;&=\; \sum_{k=1}^{4} \left(\frac{z_k^2 \;-\; \delta z_k \;+\; \omega^2}{\delta z_k}\right) C_k e^{\,-z_k t} \end{aligned} \tag{III-7}$$

Considering C_k as functions of t, and substituting Eqs. (III-7) into Eqs. (III-2, III-3) the method of variation of constants leads to the relations:

$$\sum_{1}^{4} \dot{C}_k e^{-z_k t} \;=\; 0 \tag{III-8}$$

$$\sum_{1}^{4} \frac{(z_k^2 \;-\; \delta z_k \;+\; \omega^2)}{\delta z_k}\, \dot{C}_k e^{-z_k t} \;=\; 0 \tag{III-9}$$

$$\sum_{1}^{4} -\, z_k\, \dot{C}_k e^{-z_k t} \;=\; \frac{S}{m_n} \tag{III-10}$$

$$\sum_{1}^{4} -\, z_k\, (z_k^2 \;-\; \delta z_k \;+\; \omega^2)\cdot \dot{C}_k e^{-z_k t} \;=\; \frac{S}{\bar{m}_n} \tag{III-11}$$

Eqs. (III-8)–(III-11) are four simultaneous non-homogeneous algebraic equations which may be solved for the functions $\dot{C}_k(t)$. Integration of these results gives the functions $C_k(t)$, which when substituted into Eq. (III-7) yield the response of the structure. The form of the integrals appearing in these equations will depend upon the nature of the roots of Eq. (III-5) which may appear in three combinations:

a) four real roots
b) two real and two complex roots
c) four complex roots.

For small values of n a simplification may be effected. If the frequency ω of the primarily inextensional mode is sufficiently small, the term $\omega^2 q$ in Eq. (III-2) may be neglected. When n = 1, the inextensional frequency is already equal to zero. Hence Eqs. (III-2)-(III-3) become:

$$\ddot{q} + \delta (\dot{q} + \dot{\bar{q}}) = \frac{S}{m_n} \tag{III-12}$$

$$\ddot{\bar{q}} + \bar{\delta} (\dot{q} + \dot{\bar{q}}) + \bar{\omega}^2 \bar{q} = \frac{S}{\bar{m}_n} \tag{III-13}$$

and the corresponding characteristic equation:

$$z [z^3 - (\delta + \bar{\delta}) z^2 + \bar{\omega}^2 z - \delta \bar{\omega}^2] = 0 \tag{III-14}$$

separates into:

$$z_1 = 0 \tag{III-15}$$

$$z_k^3 - (\delta + \bar{\delta}) z_k^2 + \bar{\omega}^2 z_k - \delta \bar{\omega}^2 = 0 \quad (k = 2,3,4) \tag{III-16}$$

The corresponding values of μ_k are:

$$\mu_1 = 0$$

$$\mu_k = \frac{z_k}{\delta} - 1 \quad (k = 2,3,4) \tag{III-17}$$

Hence:

$$q = C_1 + \sum_2^4 C_k e^{-z_k t}$$

$$\bar{q} = \sum_2^4 \left(\frac{z_k}{\delta} - 1\right) C_k e^{-z_k t} \tag{III-18}$$

The method of variation of constants yields the values of C_k:

$$C_2 = -\frac{\eta_2}{\rho a z_2} \int_o^t S(\lambda)\, e^{z_2 \lambda}\, d\lambda$$

$$C_3 = -\frac{\eta_3}{\rho a z_3} \int_o^t S(\lambda)\, e^{z_3 \lambda}\, d\lambda \tag{III-19}$$

$$C_4 = -\frac{\eta_4}{\rho a z_4} \int_o^t S(\lambda)\, e^{z_4 \lambda}\, d\lambda$$

$$C_1 = \left[\frac{\eta_2}{\rho a z_2} + \frac{\eta_3}{\rho a z_3} + \frac{\eta_4}{\rho a z_3} \right] \int_o^t S(\lambda)\, d\lambda$$

where

$$\eta_2 = \frac{\rho a z_2 \left[z_3\delta + z_4\delta - z_3 z_4 - \delta^2 (1 + \frac{m_n}{\bar{m}_n}) \right]}{m_n \delta (z_2 - z_3)(z_4 - z_2)} \tag{III-20a}$$

$$\eta_3 = \frac{\rho a z_3 \left[z_2\delta + z_4\delta - z_2 z_4 - \delta^2 (1 + \frac{m_n}{\bar{m}_n}) \right]}{m_n \delta (z_4 - z_3)(z_3 - z_2)} \tag{III-20b}$$

$$\eta_4 = \frac{\rho a z_4 \left[z_2\delta + z_3\delta - z_2 z_3 - \delta^2 (1 + \frac{m_n}{\bar{m}_n}) \right]}{m_n \delta (z_4 - z_3)(z_2 - z_4)} \tag{III-20c}$$

Differentiation of Eq. (III-18) yields the velocities of the inextensional and extensional responses:

$$\dot{q} = \sum_2^4 - z_k C_k e^{-z_k t}$$

$$\dot{\bar{q}} = \sum_2^4 - z_k \left(\frac{z_k}{\delta} - 1\right) C_k e^{-z_k t} \tag{III-21}$$

Substitution of Eqs. (III-19) into Eqs. (III-21) and a change of variables from λ to:

$$\gamma = \cos^{-1}(1 - c\lambda/a) \tag{III-22}$$

yields:

$$\frac{\rho c}{p}\dot{q} = \eta_2 e^{z_2 \frac{a}{c}\cos\alpha} \int_0^{\alpha} \frac{S(\gamma)}{p} \sin\gamma\, e^{-z_2 \frac{a}{c}\cos\gamma}\, d\gamma$$

$$+ \eta_3 e^{z_3 \frac{a}{c}\cos\alpha} \int_0^{\alpha} \frac{S(\gamma)}{p} \sin\gamma\, e^{-z_3 \frac{a}{c}\cos\gamma}\, d\gamma \tag{III-23}$$

$$+ \eta_4 e^{z_4 \frac{a}{c}\cos\alpha} \int_0^{\alpha} \frac{S(\gamma)}{p} \sin\gamma\, e^{-z_4 \frac{a}{c}\cos\gamma}\, d\gamma$$

where

$$\alpha = \cos^{-1}\left(1 - \frac{ct}{a}\right) \tag{III-24}$$

A similar substitution and transformation in Eqs. (III-18) and (III-21) yields expressions for q, $\bar{q}$, and $\dot{\bar{q}}$ respectively.

During the time of transit ($0 \leq \alpha \leq \pi$, $0 \leq t \leq \frac{2a}{c}$) of the shock wave front across the shell, the integrals in Eq. (III-23) are incomplete Bessel integrals. These functions do not appear to be tabulated,

but the integrations can be performed numerically without difficulty. Upon and after full envelopment ($t \geq \frac{2a}{c}$), the integrals have the following forms:

$$\int_0^{\pi} \gamma \sin\gamma\, e^{-z\cos\gamma}\, d\gamma = \frac{\pi}{z}\left[e^{z} - I_o(z)\right]$$

$$\int_0^{\pi} \sin^2\gamma\, e^{-z\cos\gamma}\, d\gamma = \frac{\pi}{z} I_1(z)$$

$$\int_0^{\pi} \sin 2\gamma \sin\gamma\, e^{-z\cos\gamma}\, d\gamma = -\frac{2\pi}{z} I_2(z) \qquad \text{(III-25)}$$

$$\int_{\pi}^{\alpha} \sin\gamma\, e^{-z\cos\gamma}\, d\gamma = \frac{1}{z}\left(e^{-z\cos\alpha} - e^{z}\right)$$

$$\frac{\pi}{p}\int_0^{\pi} S_n(\gamma) \sin\gamma\, e^{-z_k\cos\gamma}\, d\gamma = \frac{2\pi(-1)^n}{z_k}\left[I_n'(z_k) - I_n(z_k)\right] \qquad n \geq 2$$

Hence, for $t \geq 2a/c$, the inextensional component of the velocity becomes:

$$\frac{\rho c}{p}\dot{q}_1 = \frac{\eta_2 c}{z_2 a}\left[1 - e^{\frac{z_2 a}{c}\cos\alpha}\left[I_o\left(\frac{z_2 a}{c}\right) - 2I_1\left(\frac{z_2 a}{c}\right) + I_2\left(\frac{z_2 a}{c}\right)\right]\right]$$

$$+ \frac{\eta_3 c}{z_3 a}\left[1 - e^{\frac{z_3 a}{c}\cos\alpha}\left[I_o\left(\frac{z_3 a}{c}\right) - 2I_1\left(\frac{z_3 a}{c}\right) + I_2\left(\frac{z_3 a}{c}\right)\right]\right] \qquad \text{(III-26)}$$

$$+ \frac{\eta_4 c}{z_4 a}\left[1 - e^{\frac{z_4 a}{c}\cos\alpha}\left[I_o\left(\frac{z_4 a}{c}\right) - 2I_1\left(\frac{z_4 a}{c}\right) + I_2\left(\frac{z_4 a}{c}\right)\right]\right]$$

$$\frac{\rho c}{p}\dot{q}_n = 2\frac{\eta_2 c}{z_2 a} e^{\frac{z_2 a}{c}\cos\alpha}\left[I_n'\left(\frac{z_2 a}{c}\right) - I_n\left(\frac{z_2 a}{c}\right)\right]$$

$$+ 2\frac{\eta_3 c}{z_3 a} e^{\frac{z_3 a}{c}\cos\alpha}\left[I_n'\left(\frac{z_3 a}{c}\right) - I_n\left(\frac{z_3 a}{c}\right)\right] \qquad n \geq 2 \qquad \text{(III-27)}$$

$$+ 2\frac{\eta_4 c}{z_4 a} e^{\frac{z_4 a}{c}\cos\alpha}\left[I_n'\left(\frac{z_4 a}{c}\right) - I_n\left(\frac{z_4 a}{c}\right)\right]$$

Similar expressions apply for q, $\bar{q}$, and $\dot{\bar{q}}$.

The various results given are suitable for computations only if Eq. (III-16) has three real roots. This equation may have one real and two complex roots, in which case more suitable expressions are given in reference 3.

The components of the acceleration are obtained from Eqs. (III-12) (III-13) once $\dot{q}$, $\bar{q}$, and $\dot{\bar{q}}$ have been evaluated:

$$2\frac{\rho a}{p}\ddot{q}_n = 2\frac{\rho a}{m_n}\frac{S_n}{p} - 2\frac{\rho a}{m_n}\frac{\rho c}{p}(\dot{q}_n + \dot{\bar{q}}_n) \qquad \text{(III-28)}$$

$$2\frac{\rho a}{p}\ddot{\bar{q}}_n = 2\frac{\rho a}{\bar{m}_n}\frac{S_n}{p} - 2\frac{\rho a}{\bar{m}_n}\frac{\rho c}{p}(\dot{q}_n + \dot{\bar{q}}_n) - 2\left(\frac{\bar{\omega}_n a}{c}\right)^2\frac{\rho c^2}{pa}\bar{q}_n \qquad \text{(III-29)}$$

where $\frac{p}{2\rho a}$ is the average acceleration during the transit time, that would produce a shell velocity equal to the particle velocity in the shock wave.

The pressure of the fluid on the shell,

$$Z_n = Q_n \cos n\theta \qquad \text{(III-30)}$$

is found by means of Eqs. (II-21 and (III-12) from:

$$\frac{Q_n}{p} = \frac{m_n}{p}\ddot{q}_n \qquad \text{(III-31)}$$

and is proportional to the primarily inextensional component of the acceleration.

The direct stress (hoop stress) in the shell is obtained by the relation:

$$\sigma = \frac{E}{(1-\nu^2)}\epsilon \qquad \text{(III-32)}$$

where

$$\epsilon = \frac{1}{a}\left(-w + \frac{\partial \nu}{\partial \theta}\right). \qquad \text{(III-33)}$$

Using Eqs. (II-3) and (II-4) the n - th component of the direct stress becomes:

$$\sigma = \frac{-E}{(1-\nu^2)a}(n^2+1)\bar{q}_n \cos n\theta = \frac{-ma}{h}\left[\frac{\ddot{q}}{n^2} - \ddot{\bar{q}}\right]\cos n\theta \qquad \text{(III-34)}$$

The n - th component of the flexural stress σ_B is obtained from

$$\sigma_B = \frac{-(n^2-1)Ed}{a^2}(q_n + \bar{q}_n)\cos n\theta. \qquad \text{(III-35)}$$

IV Accuracy of the Approximation, Eq. (II-20).

The approximation, Eq. (II-20), which has been derived in reference 1 is valid for short times after the impact of the wave. It is applicable only for such values of the time t where

$$H_n^{(2)}\left(\frac{\pi a}{ct}\right) \simeq i\, H_n'^{(2)}\left(\frac{\pi a}{ct}\right) . \tag{IV-1}$$

The approximation is good for large values of the argument of the Hankel Functions, but it depends on the value of n how large it must be.

For $n = 0$ the approximation is still meaningful at the end of the transit time. At this time the value of the argument is $\pi/2$ and the error is about 10%. However, for $n > 1$, the error increases and the results at transit time or later are certainly not applicable. This is fortunately not too serious because the major effects in the higher modes occur within a rather short time.

To obtain a criterion for judging the accuracy of the numerical results for $n = 1$ given in this paper, one can compare the values of the approximate solutions for $t \to \infty$ and the asymptotic values obtainable from the solution of the problem by integral transforms[1] in reference 2. The theory of this paper gives

$$\lim_{t \to \infty} \dot{q}_1 = \frac{P}{\rho c} . \tag{IV-2}$$

while the value obtained by asymptotic integration of the results of reference 2 is[2]

$$\lim_{t \to \infty} \dot{q}_1 = \frac{P}{\rho c} \cdot \frac{2}{1 + \frac{2m}{\rho a}} \tag{IV-3}$$

The two values agree only if $\frac{\rho a}{2m} = 1$, i.e. for a neutrally buoyant shell. Due to the fact that the important peak accelerations occur at early times it is likely that the difference in the velocity at $t \to \infty$ does not affect these accelerations.

v) Comparison of Results of Extensional and Inextensional Theories

To illustrate the extensional effects, response curves for $n = 1$ and 2 were obtained and can be compared with the results found from the inextensional theory, reference 1. To be able to combine the response from the various modes, it is necessary to use consistent values of the frequencies. The selected values representing steel shells in water, are

$$\bar{\omega}_n = \frac{10}{3} (n^2 + 1) \frac{c}{a} \tag{V-1}$$

Two cases were considered for $n = 1$ in order to show that the extensional effects are more pronounced for light shells than for buoyant ones.

---

(1) This solution did not include extensional effects, but this should be immaterial.

(2) This result was previously obtained by Dr. W. T. Settee using quite simple impulse considerations; the asymptotic integration which does not present any fundamental difficulty, was made to confirm this result.

a) Buoyant Shell, $\frac{\rho a}{2m} = 1$, $n = 1$

Figure 2 shows the extensional effect on the velocity component $\dot{q}_1$ to be small; it also shows $\dot{\bar{q}}_1$ which has no counterpart in the inextensional theory. Fig. 3 compares the accelerations and the fluid pressures Q_1. The combinations of the accelerations $\ddot{q}_1$ and $\ddot{\bar{q}}_1$ give the acceleration of points on the surface of the shell:

$$w = (\ddot{q}_1 + \ddot{\bar{q}}_1) \cos \theta \qquad \text{(V-2)}$$

For neutral buoyancy, the fluid pressure Q_1 does not change significantly due to extensional effects. Furthermore, the acceleration $\ddot{q}_1$ which describes the rigid body motion of the entire shell is only slightly affected.

To obtain a comparison of the acceleration $\ddot{w}$ of the surface of the shell, Fig. 4 gives $\ddot{w}$ (0,t), i.e. $\ddot{w}$ for $\theta = 0$. It is seen that the peak of the extensional response is nearly one third larger than the inextensional one. It should be noted however, that the area under the $\ddot{w}$ curve, i.e. the impulse imparted to an element of the shell, is about the same for both theories.

Fig. 5 finally shows the ratio of the direct circumferential stress to the hoop stress $\sigma^* = -pa/h$ due to a static pressure of intensity p.

The extensional curves have a heavily damped oscillatory character not shown by those from the inextensional theory. This is clearly due to the influence of the extensional vibrations of the shell.

b) Light Shell, $\frac{\rho a}{2m} = 5$, $n = 1$

Figures 6 to 9 show the corresponding curves for a shell whose mass is only one fifth of that of the displaced medium. It is quite apparent that the differences between extensional and inextensional theory are larger than that for the buoyant shell. All the curves again have a heavily damped oscillatory character with the period of the extensional vibrations of the shell.

Figure 6 includes also the asymptotic value of the velocity $\dot{q}_1$ for large times according to the expression given in Section IV. It is clear that present theory breaks down at or before the end of the transit time $t = \frac{2a}{c}$. It should be stressed that the peak acceleration and the peak direct stress all occur very much earlier, and they are therefore well approximated by the present theory.

c) Light Shell, $\frac{\rho a}{2m} = 5$, $n = 2$

Figures 10–14 show curves for the $n = 2$ mode for the light shell already considered in case b. Fig. 10 shows the ratio of the maximum flexural stress σ_B to the hoop stress σ^*.

The extensional effect on the flexural stress is very small and the inextensional theory curve is indistinguishable from that of the present theory.

Figure 11 shows the extensional effect on the velocity component $\dot{q}_2$ to be fairly small, it also shows $\dot{\bar{q}}_2$ which has no counterpart in the inextensional theory. Figure 12 shows the accelerations and the fluid pressure Q_2. The fluid pressure Q_2 is only slightly affected by the extensional effects. The acceleration components $\ddot{q}_2$ and $\ddot{\bar{q}}_2$ by themselves have no physical significance but their combination gives the acceleration of points on the surface of the shell:

$$w = (\ddot{q}_2 + \ddot{\bar{q}}_2) \cos 2\theta \qquad \text{(V-3)}$$

Figure 13 shows the acceleration of the shell at $\theta = 0$, i. e. $\ddot{w}$ (0,t). The peak of the extensional response

is increased by about 20% over the inextensional one. Again, the impulse imparted to an element of the shell is about the same for both theories. Figure 14 finally shows the ratio of the direct circumferential stress to the hoop stress σ^*.

Again, due to the influence of the extensional vibrations of the shell, all the extensional curves have a damped oscillatory character not shown by the inextensional theory. The damping is much less pronounced for this mode than for the mode n = 1.

VI. Shell with an Additional Mass

It is possible to treat the slightly more general case of a cylindrical shell with an additional mass M (per unit length) on the axis in a similar manner as the plain cylindrical shell. The mass is assumed to be connected to the shell by "uniformly distributed" springs having a spring constant K (per unit of area of the shell), Fig. (15). To show that the interaction problem leads to similar equations as in the case without the mass M treated before, the modes in vacuo are required. For simplicity only the case of an inextensional shell is considered. The kinetic and potential energies per unit length of shell are:

$$T = \frac{m}{2}\int_o^{2\pi} (\dot{w}^2 + \dot{v}^2)\ a d\theta + \frac{1}{2} M\dot{x}^2 \tag{VI-1}$$

$$V = \frac{EI}{2a^3}\int_o^{2\pi} (w_{\theta\theta} + w)^2\ d\theta + \frac{Ka}{2}\int_o^{2\pi} (x\cos\theta - w)^2\ d\theta$$

where x is the displacement of the mass M. For an inextensional shell the condition

$$w = v_\theta \tag{VI-2}$$

must be satisfied. The differential equations of motion can be obtained from Hamilton's Principle; these differential equations can be solved by general expressions

$$\begin{aligned} w &= q_n \cos n\theta\, e^{i\omega_n t} \\ v &= \frac{1}{n} q_n \sin n\theta\, e^{i\omega_n t} \\ x &= X_n\ q_n\, e^{i\omega_n t} \end{aligned} \tag{VI-3}$$

where it is found that the displacement x vanishes except for n = 1; in other words the motion of the mass does not couple with the modes for $n \neq 1$ at all. The only effect of the mass is a slight change in the frequencies due to the springs K. The solutions for $n \geq 2$ found in reference 1 apply therefore for the new system, provided the frequencies are modified; if extensional results are included it can be shown similarly that the results of Section III apply, except for n = 1.

For the case n = 1 (inextensional) two modes exist, having the respective frequencies

$$\begin{aligned} \omega_1^2 &= 0 \\ \bar{\omega}_1^2 &= \frac{K}{2}\left(\frac{1}{m} + \frac{2a\pi}{M}\right) \end{aligned} \tag{VI-4}$$

The frequency $\omega_1 = 0$ pertains to a rigid body motion, similar to the one found previously for n = 1; the shape of the mode being

$$w = \cos\theta, \quad v = \sin\theta, \quad X_1 = 1 \qquad \text{(VI-5)}$$

The shape of the mode for the other frequency is

$$w = \cos\theta, \quad v = \sin\theta, \quad X_1 = -\frac{2a\pi m}{M} \qquad \text{(VI-6)}$$

It is a relative motion of the mass M and the shell, without change of shape of the shell[1]. The values of the generalized masses for these modes are:

$$m_1 = 2m\left(1 + \frac{M}{2a\pi m}\right)$$

$$\bar{m}_1 = 2m\left(1 + \frac{2a\pi m}{M}\right) \qquad \text{(VI-7)}$$

The w component of the new mode shapes, Eqs. (VI-5,6), does not differ from that of Eqs. (II-1, 2), and the solution of the interaction problem for the inextensional shell with the added mass is formally identical with the solution already found for the extensional shell without the mass in the case n = 1. It is simply necessary to use the appropriate values of the frequencies and generalized masses.

The extensional case could also be treated, but leads to three simultaneous differential equations of the type (II-6, 7). If the frequency $\bar{\omega}_1$ according to Eq. (VI-4) is sufficiently smaller than the extensional frequency of the shell there will be little coupling, and the acceleration of the mass M can be found with good approximation from the inextensional analysis.

Fig. 16 shows the acceleration $\ddot{x}$ of the mass at the center for the case of a light shell, $\frac{\rho a}{2m} = 5$, where the additional mass $M = 8\pi am$ is selected to make the structure neutrally buoyant; a rather stiff spring was selected giving $\bar{\omega}_1 = 1.00\frac{c}{a}$, about one third of the extensional frequency $\bar{\omega}_0 = 3.33\frac{c}{a}$. Only the portion of the curve $\frac{ct}{2a} \geq 1$ which follows from the closed expressions (III-26) is shown; the portion $\frac{ct}{2a} < 1$ would have required additional numerical integrations which were thought unwarranted, as the maximum value of $\ddot{x}$ occurs for $\frac{ct}{2a} > 1$. In spite of the stiff spring, it is seen that the largest acceleration of the mass M is considerably reduced and its occurrence delayed compared to the values of the accelerations $\ddot{w}(0,t)$ on the surface of the shell; Fig. 16 indicates for this purpose the $\ddot{w}$ curves found previously for a light and for a buoyant shell without center mass M. A similar computation for the case $\bar{\omega}_1 = 0.10\frac{c}{a}$ shows a reduction of the acceleration to max. $\ddot{x} \simeq 0.03\frac{p}{\rho a}$ indicating the protection against shock effects which can be obtained by shock mountings.

VII Summation of Effects from all Modes: Pressure of Medium

To obtain the actual physical effect of the shock wave it is necessary to add the contributions from all modes. While it is correct that for a step wave and for large values of the time t the lowest modes n = 0 and 1 will be dominant, this is not the case for very small values of t where the higher modes remain important. It is, therefore, of considerable interest to realize that there is a possibility of actually summing the contributions for different n. This question will be studied in the next two sections.

---

(1) This is of course due to the assumed inextensionality.

A very interesting result which is obviously valid for any shape of the structure, not only for cylindrical shells, can be obtained by considering the pressure Z of the medium on the shell. Substituting Eq. (II-21) into Eq. (II-5) gives

$$Z = \sum_{n=0}^{\infty} P_n(t) \cos n\theta + \sum_{n=0}^{\infty} V_n(t) \cos n\theta - \rho c \sum_{n=0}^{\infty} (\dot{q}_n + \dot{\bar{q}}_n) \cos n\theta \qquad \text{(VII-1)}$$

Each of these sums can be recognized:the first one is the pressure in the shock wave, $p(\theta,t)$, see Eq. (II-12), the second one is a multiple of the radial component of the particle velocity in the shock wave, $\rho c\, v(\theta,t) = \cos\theta\, p(\theta,t)$, Eq. (II-18); the last one is the radial velocity, $\dot{w}(\theta,t)$. The fluid pressure is therefore

$$Z(\theta,t) = (1 + \cos\theta)\, p(\theta,t) - \rho c\, \dot{w}(\theta,t) \qquad \text{(VII-2)}$$

This relation expresses the fluid pressure at a given point solely as function of the incident pressure $p(\theta,t)$ and of the velocity $\dot{w}(\theta,t)$ of the point at which the pressure acts. Within the limit of validity of this equation, i.e. for small values of t, this relation permits the direct writing of the differential equations of motions of the structure; the equation of motion of the fluid no longer appears.

The derivation of Eq. (VII-2) is possible because of the approximation, Eqs. (3-9), in reference 1 which results in the pressure Z at any point of the shell becoming independent from whatever happens at other points of the shell; it can therefore not matter if the structure at those other points would not be a cylindrical shell, and one can use the approximation Eq. (VII-2) therefore on any other submerged structure. Its use is an enormous simplification of the task of finding the response of a structure to a shock wave. The result can of course only be valid for the early part of the interaction problem.

When Eq. (VII-2) is applied to problems of skew incidence of a shock wave on a cylindrical shell, or to evaluate the effect of a shock wave on the end section of a shell, the angle θ must be clearly defined. It is the angle between the direction of propagation of the shock wave and the inner normal of the surface.

VIII Total Acceleration, Stress and Fluid Pressure for Small Values of t

The expression (VII-2) obtained in the previous section will be used to obtain approximations for the total values due to all modes of the acceleration, the direct stress, and the fluid pressure for small values of the time t.

Consider the motion of the shell, Fig. 17, under the action of normal forces $Z(\theta,t)$ defined by Eq. (VII-2). For analysis purposes a section of the shell of unit length in the direction of the shell axis is studied. This section forms a ring, similar to the one considered in the Appendix. For small values of the time t the extensional forces in the ring will be dominant, while the bending effects are very small. As the following analysis is only intended for small values of t the bending stiffness will be entirely neglected to simplify the computations. The equations of motion of an elastically compressible ring without bending stiffness due to a system of radial forces $Z(\theta,t)$ are

$$m\ddot{w} + \frac{EA}{a^2}(w - v_\theta) = Z$$

$$m\ddot{v} + \frac{EA}{a^2}(w_\theta - v_{\theta\theta}) = 0 \qquad \text{(VIII-1)}$$

Substituting Eq. (VII-2) for Z the equations of motion may be written in the form

$$\ddot{w} + \frac{\rho c}{m} \dot{w} = \frac{p(\theta,t)\,(1 + \cos\theta)}{m} - \frac{EA}{ma^2}(w - v_\theta)$$

$$\dot{v} = -\frac{EA}{ma^2}(w_\theta - v_{\theta\theta}) \qquad \text{(VIII-2)}$$

The last term in the first Eq. (VIII-2) is proportional to the hoop strain $\epsilon = \frac{1}{a}(w - v_\theta)$; it is physically obvious that a short time after the shock wave hits the shell the strain must be compressive, $\epsilon \geq 0$. One can reason further that the strain ϵ will decrease as θ increases, giving $w_\theta - v_{\theta\theta} \leq 0$. It follows from these inequalities that the solutions $\bar{w}$ and $\bar{v}$ of the differential equations (VIII-2, 3) without the extensional terms

$$\ddot{\bar{w}} + \frac{\rho c}{m} \dot{\bar{w}} = \frac{p(\theta,t)\,(1 + \cos\theta)}{m}$$

$$\ddot{\bar{v}} = 0 \qquad \text{(VIII-3)}$$

will give upper limits for w, but lower limits for v, or their derivatives. A solution based on Eq. (VIII-3) will give therefore upper limits not only foı the radial acceleration $\ddot{w}$, but also for the hoop strain and stress which are proportional to $w - v_\theta$; it will also give an upper limit for the pressure $Z(\theta,t)$ provided[1] it is determined from the first of the Eqs. (VIII-1).

It is possible to refine the above considerations and obtain a criterion for the length of time for which the approximate Eqs. (VIII-3) give the upper limits described. One significant fact typical for the conditions for very small values of t is that the shell ahead of the wave front A-A, Fig. 18, must be at rest and strainless. This is so because during the time dt it takes the wave front to progress from A to B a compressive wave in the shell will have progressed a distance $c_s dt$ from A towards B, where c_s is the velocity of sound in the shell. If the angle θ is small the compressive wave in the shell will reach point B later than the wave in the fluid and the shell ahead of the wave front will be undisturbed. This will be the case if the time is so short that $\theta \leq \theta_L$ where the limiting angle is defined by

$$\theta_L = \sin^{-1}(c/c_s) \simeq c/c_s \qquad \text{(VIII-4)}$$

The limiting value t_L of the time where this occurs is

$$t_L = \frac{a}{c}(1 - \cos\theta_L) \simeq \frac{c^2}{4c_s^2}\,\frac{(2a)}{c} \qquad \text{(VIII-5)}$$

It is now intended to ascertain that Eqs. (VIII-3) furnishe the described limits by showing that

---

(1) A lower limit for $Z(\theta,t)$ is obtained if it is determined from Eq. (VII-2). One can also obtain a lower limit for $\ddot{w}$ by using Eq. (VIII-2) in the form

$$\ddot{w} = \frac{p(\theta,t)\,(1 + \cos\theta)}{m} - \frac{\rho c}{m}\dot{\bar{w}} - \frac{EA}{ma^2}(\bar{w} - \bar{v}_\theta)$$

for $t \leq t_L$ the neglected term $w - v_\theta$ is positive. Defining a new "local" time τ for each point of the shell such that the arrival of the shock wave occurs at $\tau = 0$

$$\tau = t - \frac{a}{c}(1 - \cos\theta) \tag{VIII-6}$$

the pressure can be defined by

$$p(\theta,\tau) = \begin{cases} 0 & \text{if } \tau < 0 \\ p(\tau) & \text{if } \tau \geq 0 \end{cases} \tag{VIII-7}$$

where $p(\tau)$ describes the shape of the shock wave.

Since for $t < t_L$ the points of the shell are undisturbed prior to the arrival of the wave front, the displacements w and v can be expanded for $\tau \geq 0$ in a Taylor series in ascending powers of τ. Because of the rest conditions for $\tau = 0$ the lowest terms of the series will be τ^2,

$$w = \sum_{j=2} \tau^j f_{j(\theta)} \tag{VIII-8}$$

$$v = \sum_{j=2} \tau^j g_j(\theta) \tag{VIII-9}$$

Substituting Eq. (VIII-8) and Eq. (VIII-9) into Eq. (VIII-2) the functions $f_j(\theta)$ and $g_j(\theta)$ may be evaluated by equating coefficients. Using terms up to τ^3, the approximate expression for $w - v_\theta$ becomes

$$w - v_\theta = \frac{p(\theta,t)(1+\cos\theta)}{2m}\left\{\frac{\tau^2}{L} - \frac{\tau^3 c}{aL}\left(\frac{\rho a}{3m} + \frac{c_s^2\cos\theta}{3c^2} + \frac{4c_s^6\sin^4\theta\cos\theta}{3c^6L^2} + \frac{5c_s^4\sin^2\theta\cos\theta}{3c^4L}\right)\right\}$$

$$+ \frac{p(\theta,t)\, c_s^2 \sin^2\theta\, \tau^3}{3m\, cL^2 a} \tag{VIII-10}$$

where $L = 1 - \frac{c_s^2}{c^2}\sin^2\theta$.

For the extreme case of $\theta = 0$, and $\tau = t_L$, Eq. (VIII-10) becomes

$$w - v_\theta = \frac{p(\theta,t)}{m}\tau^2\left(\frac{5}{6} - \frac{1}{6}\frac{c^2}{c_s^2}\frac{\rho a}{m}\right) \tag{VIII-11}$$

and $w - v_\theta$ will be positive provided

$$\frac{\rho a}{m} \leq \frac{5c_s^2}{c^2} \tag{VIII-12}$$

For the case of steel shells in water, $\frac{c_s^2}{c^2} \simeq 10$, the above analysis will be valid if $t \leq t_L = \frac{1}{40}$ of transit time and $\frac{\rho a}{2m} \leq 25$.

Therefore, for times up to about 1/40 of full envelopement (and presumably somewhat later), an upper limit for the acceleration and stress can be obtained from an analysis based on Eqs. (VIII-3), for all but extremely light shells.

For the case of a step wave, Eq. (VIII-3) yields the solution

$$\bar{w} = \frac{p(1+\cos\theta)}{\rho c}\left[\frac{m}{\rho c}\left(e^{\frac{-\rho c}{m}t} - 1\right) + t\right] \qquad \text{(VIII-13)}$$

The peak value of the total acceleration $\ddot{\bar{w}}$ is quite high but $\dddot{\bar{w}}$ decays extremely fast. For small values of θ, $\theta \tilde{<} 0$,

$$\dddot{\bar{w}} = \frac{2p}{m} e^{-\frac{\rho c}{m}t} \qquad \text{(VIII-14)}$$

which is the solution for the case of a plane shock wave hitting an air backed flat plate of mass m.

The upper limit for the direct (hoop) stress in the shell at $\theta = 0$ is given by

$$\frac{\sigma}{\sigma^*} = \frac{2m}{\rho a}\left(\frac{\bar{\omega}_o a}{c}\right)^2\left[\frac{m}{\rho a}\left(e^{\frac{-\rho c}{m}t} - 1\right) + \frac{ct}{a}\right] \qquad \text{(VIII-15)}$$

The upper limits for the acceleration $\ddot{w}$ and direct stress, although valid only for small t, are of value in judging the convergence of the mode approach. Fig. 19 shows the components of the acceleration $\ddot{w}$ at $\theta = 0$ for n = 0, 1 and 2 for the thin shell considered earlier. While $\ddot{w}_2$ is slightly smaller than $\ddot{w}_1$ one can not speak of convergence, and more terms are obviously required to obtain a meaningful result. This is borne out by Fig. 20 which shows the summation curve and the upper limit approximation for $\ddot{w}$ obtained from Eq. (VIII-14). The latter may be used to compute $\ddot{w}$ up to about ct/2a = 0.05; for larger t the mode approach ought to give reasonable results without using an excessive number of terms. It will be noted that the area of the two curves in Fig. 20, representing the total impulse, differs not very much.

Fig. 21 shows the components of the hoop stress σ for n = 0, 1 and 2, the sum of these components, and the upper limit for the total stress for small values of t. The convergence of the stress components is quite good for ct/2a > 0.1, i.e. for the range where the total stresses are large. For smaller values of t the approximate upper limit is available, but it is unimportant as the largest stresses for a step shock of long duration occur much later, when the mode approach converges well. It is quite obvious that the significant part of the stress is due to the n = 0 and 1 modes. The mode approach is therefore quite satisfactory for the stress problem for shock waves of long duration. For short duration shocks, say 1/20 of the transit time or less, on the other hand the approximate solution is appropriate as being more accurate and much simpler.

Fig. 22 shows the components Q_n of the fluid pressure. Convergence is reasonable except for small values of t. Fig. 23 shows the upper limit according to Eq. (VIII-1) which indicates a rapid decrease of the pressure Z = 2p for t = 0. For ct/2a = 0.10 the upper limit and the sum of the first three components are about alike indicating that the mode approach is reasonable for larger values of t.

References

1. R. D. Mindlin and H. H. Bleich, "Response of an Elastic Cylindrical Shell to a Transverse Step Shock Wave," Journal of Applied Mechanics, Vol. 20, No. 2 June 1953, p. 189.

2. G. F. Carrier, "The Interaction of an Acoustic Wave and an Elastic Cylindrical Shell," Contract N7 onr – 35810, Technical Report No. 4, Brown University R.I., October 1951.

3. M. L. Baron, "A Further Study of the Response of an Elastic Cylindrical Shell to a Transverse Shock Wave," Ph. D. dissertation, Columbia University, N.Y., June 1953.

APPENDIX

Free Vibrations of a Thin Circular Ring.

The following derivation differs from the usual treatment by considering simultaneously bending and extensional effects. The effects of shear and rotatory inertia are not considered, because they affect only very high modes not of interest here.

Let w be the radial displacement (positive inward) of a point on the center line of the ring and v be the tangential displacement (positive in the direction of increasing θ). The kinetic energy of the vibrating system is:

$$T = \frac{m}{2} \int_o^{2\pi} (\dot{w}^2 + \dot{v}^2)\, a\, d\theta \tag{A-1}$$

and the potential energy is, (using $\bar{E} = \frac{E}{(1 - \nu^2)}$ for the plane strain solution),

$$V = \frac{\bar{E}A}{2a} \int_o^{2\pi} (v_\theta - w)^2 \, d\theta + \frac{\bar{E}I}{2a^3} \int_o^{2\pi} (w_{\theta\theta} + w)^2 \, d\theta \tag{A-2}$$

where I is the moment of inertia of the cross section of the ring with respect to a principal axis at right angles to the plane of the ring.

Using Hamilton's Principle, the differential equations of motion are obtained from the condition that the integral

$$J = \int_o^t (T - V)\, dt \tag{A-3}$$

shall be stationary. Substituting Eqs. (A-1) and (A-2) in Eq. (A-3) and applying the rules of the calculus of variations, the following set of simultaneous partial differential equations is obtained:

$$\begin{aligned} -ma\ddot{w} + \frac{\bar{E}A}{a}(v_\theta - w) - \frac{\bar{E}I}{a^3}(w_{\theta\theta\theta\theta} + 2w_{\theta\theta} + w) &= 0 \\ -ma\ddot{v} + \frac{\bar{E}A}{a}(v_{\theta\theta} - w_\theta) &= 0 \end{aligned} \tag{A-4}$$

Suitable solutions of Eq. (A-4) are:

$$\begin{aligned} w &= \cos n\theta \, e^{i\omega t} \\ v &= \frac{1}{d} \sin n\theta \, e^{i\omega t} \end{aligned} \tag{A-5}$$

where n = 0, 1, 2, ... is an integral number indicating the number of circumferential waves. Substitution of Eq. (A-5) into Eq. (A-4) leads to the two homogeneous equations:

$$\left[\omega^2 - \frac{\bar{E}A}{ma^2} - \frac{EI}{ma^4}(n^2 - 1)^2\right] + \frac{1}{d}\frac{n\bar{E}A}{ma^2} = 0$$

$$\frac{n\bar{E}A}{ma^2} + \frac{1}{d}\left[\omega^2 - \frac{\bar{E}A}{ma^2}n^2\right] = 0 \qquad \text{(A-6)}$$

Non-vanishing solutions of Eqs. (A-6) and free vibrations, exist only if the determinant of Eq. (A-6) vanishes. This leads to the frequency equation:

$$\omega^4 - \omega^2\left[\frac{\bar{E}A}{ma^2}(n^2 + 1) + \frac{EI}{ma^4}(n^2 - 1)^2\right] + \frac{EI}{ma^4}\frac{\bar{E}A}{ma^2}n^2(n^2 - 1)^2 = 0 \qquad \text{(A-7)}$$

Eq. (A-7) yields two frequencies:

$$\left.\begin{matrix}\omega_n^2 \\ \bar{\omega}_n^2\end{matrix}\right\} = \left[\frac{\bar{E}A}{2ma^2}(n^2 + 1) + \frac{EI}{2ma^4}(n^2 - 1)^2\right] \mp$$

$$\mp\sqrt{\left[\frac{\bar{E}A}{2ma^2}(n^2 + 1) + \frac{EI}{2ma^4}(n^2 - 1)^2\right]^2 - \frac{EI}{ma^4}\frac{\bar{E}A}{ma^2}n^2(n^2 - 1)^2} \qquad \text{(A-8)}$$

where ω_n corresponds to a primarily inextensional mode and $\bar{\omega}_n$ to a primarily extensional mode. Substitution of these frequencies in Eq. (A-6) yields values d and $\bar{d}$ corresponding to the two frequencies. Because of the orthogonality relations between the two modes of frequency ω_n and $\bar{\omega}_n$, the relation $\bar{d}_n = -\frac{1}{d_n}$ exists where:

$$d_n = \frac{n^2 - 1}{2n} - \frac{(1 - n^2)^2}{2n}\frac{I}{a^2A} +$$

$$+\frac{1}{2}\sqrt{\left(\frac{n^2 + 1}{n}\right)^2 + \frac{2(1 - n^2)^3}{n^2}\frac{I}{a^2A} + \frac{(1 - n^2)^4}{n^2}\frac{I^2}{a^4A^2}} \qquad \text{(A-9)}$$

The displacements w and v of the primarily inextensional modes are given by:

$$w = \cos n\theta$$

$$v = \frac{1}{d_n}\sin n\theta \qquad \text{(A-10)}$$

while those of the primarily extensional modes become:

$$w = \cos n\theta$$

$$v = \frac{1}{d_n} \sin n\theta = -d_n \sin n\theta. \tag{A-11}$$

For properties of practical interest and for the lower modes ($n \leq 5$), there is little coupling between the bending and extensional effects because $a^2A >> I$; Eqs. (A-8) and (A-9) may then be approximated very closely by:

$$\omega_n^2 = \frac{EI(1 - n^2)^2 n^2}{ma^4(n^2 + 1)}$$

$$\bar{\omega}_n^2 = \frac{EA}{ma^2}(n^2 + 1) \tag{A-12}$$

and

$$d_n = n. \tag{A-13}$$

Determination of the Generalized Masses m_n and $\bar{m}_n$.

The displacement of the shell is given by Eq. (II-3) and (II-4). The kinetic energy of a section of shell of unit width for the n^{th} mode ($n \neq 0$) is:

$$T = \frac{ma\pi}{2}\left[\left(1 + \frac{1}{d_n^2}\right)\dot{q}_n^2 + (1 + d_n^2)\dot{\bar{q}}_n^2\right] \tag{A-14}$$

and the potential energy is:

$$V = \frac{EA\pi}{2a}\left[\left(\frac{1}{d_n} - 1\right)^2 q_n^2 + (d_n + 1)^2 \bar{q}_n^2\right] + \frac{EI\pi}{2a^3}(1 - n^2)^2 (q_n^2 + \bar{q}_n^2) \tag{A-15}$$

The Lagrangian equations of motion for small oscillations are:

$$\frac{\partial}{\partial t}\left(\frac{\partial T}{\partial \dot{q}_n}\right) + \frac{\partial V}{\partial q_n} = F_n \tag{A-16}$$

where F_n is the generalized force corresponding to the generalized coordinate q_n.

The force F_n can be found by the method of virtual work. Consider the n^{th} component of the radial pressure on the cylinder, (Eq. (II-5)

$$Z_n = Q_n(t) \cos n\theta. \tag{A-17}$$

Upon changing the coordinate q_n by an amount δq_n, the corresponding displacement w is:

$$w = \delta q_n \cos n\theta \tag{A-18}$$

The work done by the pressure Z_n on the above displacement becomes:

$$W = \int_0^{2\pi} Z_n \, \delta q_n \, \cos n\theta \, a d\theta \tag{A-19}$$

which when equated to $F_n \, \delta q_n$, yields the generalized force:

$$F_n = \int_0^{2\pi} Z_n \, \cos n\theta \, a d\theta = \int_0^{2\pi} Q_n \cos^2 n\theta \, a d\theta = Q_n \pi a \tag{A-20}$$

The equations of motion are obtained by applying Eq. (A-16):

$$\begin{aligned} &ma\pi \left(1 + \frac{1}{d_n^2}\right)\ddot{q}_n + ma\pi \left(1 + \frac{1}{d_n^2}\right) \omega_n^2 \, q_n = Q_n \pi a \\ &ma\pi \left(1 + d_n^2\right) \ddot{\bar{q}}_n + ma\pi \left(1 + d_n^2\right) \bar{\omega}_n^2 \, \bar{q}_n = Q_n \pi a \end{aligned} \tag{A-21}$$

where ω_n^2 and $\bar{\omega}_n^2$ are the frequencies defined by Eq. (A-8). Eqs. (A-21) may be written finally:

$$\begin{aligned} &\ddot{q}_n + \omega_n^2 \, q_n = \frac{Q_n}{m_n} \\ &\ddot{\bar{q}}_n + \bar{\omega}_n^2 \, \bar{q}_n = \frac{Q_n}{\bar{m}_n} \end{aligned} \tag{A-22}$$

where

$$\begin{aligned} m_n &= m\left(1 + \frac{1}{d_n^2}\right) \\ \bar{m}_n &= m\left(1 + d_n^2\right) \end{aligned} \tag{A-23}$$

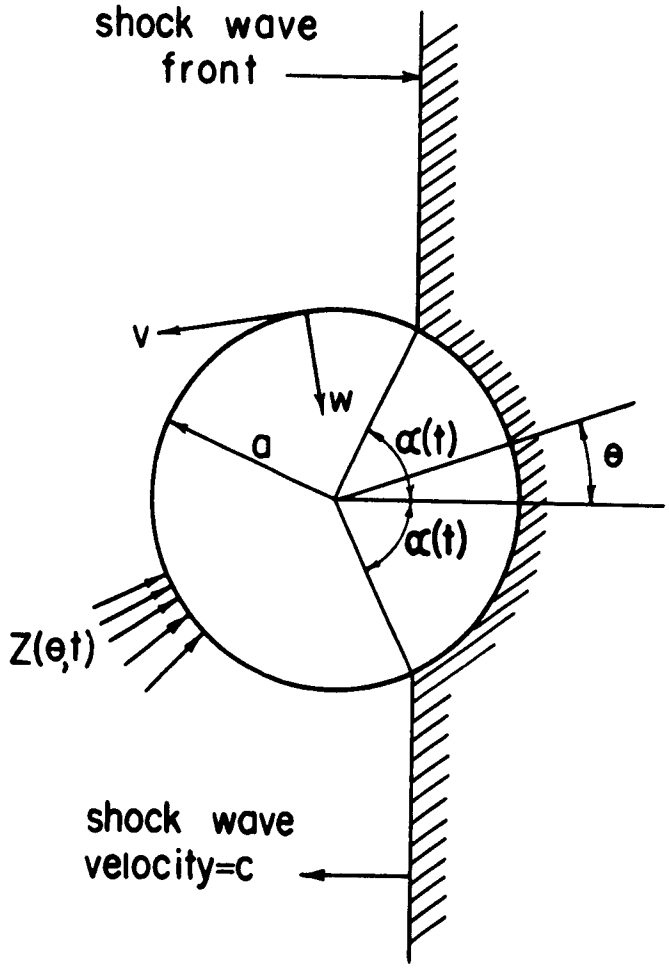

Figure 1

Geometry of Problem

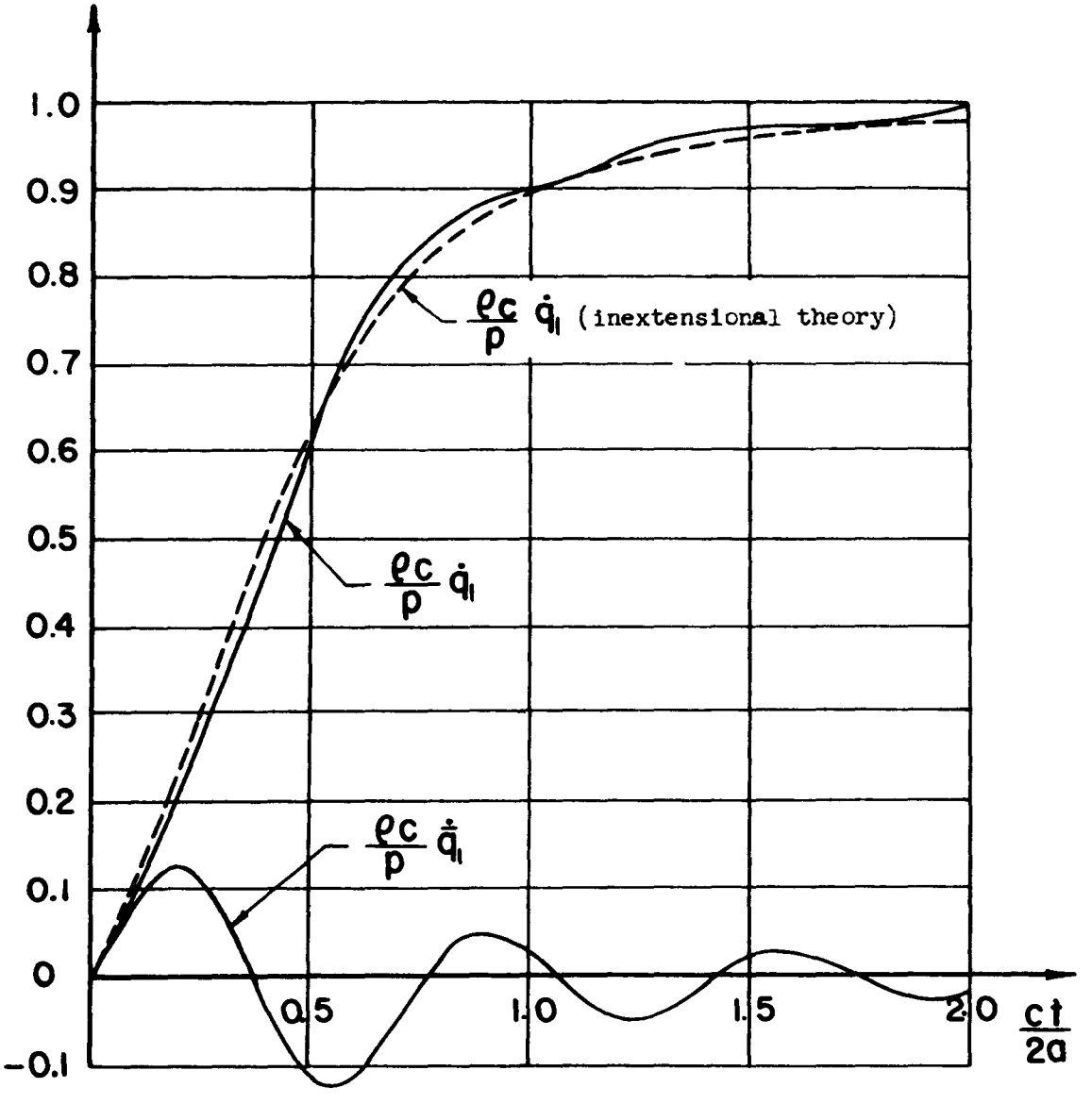

Fig. 2 Velocities $\dot{q}_1$ and $\ddot{q}_1$ (for $n = 1, \frac{\rho a}{2m} = 1$).

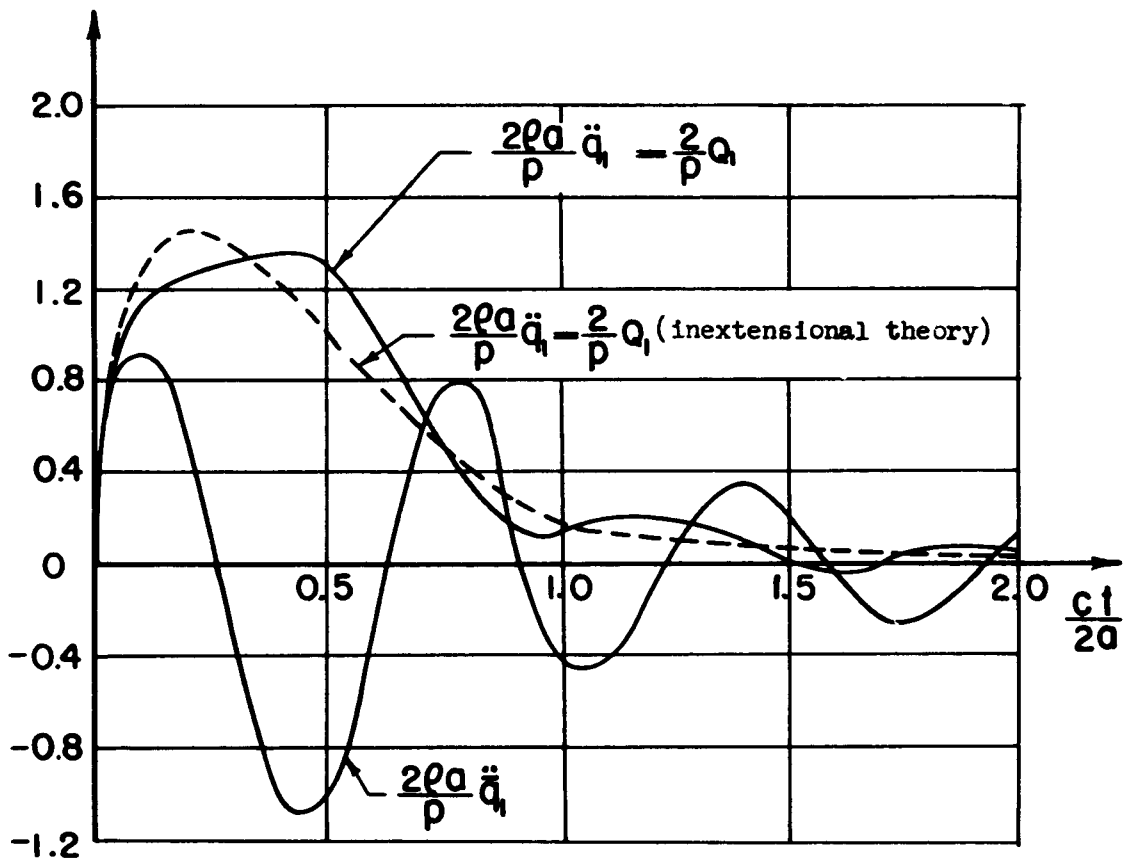

Fig. 3 Accelerations and Fluid Pressure (for $n = 1, \frac{\rho a}{2m} = 1$).

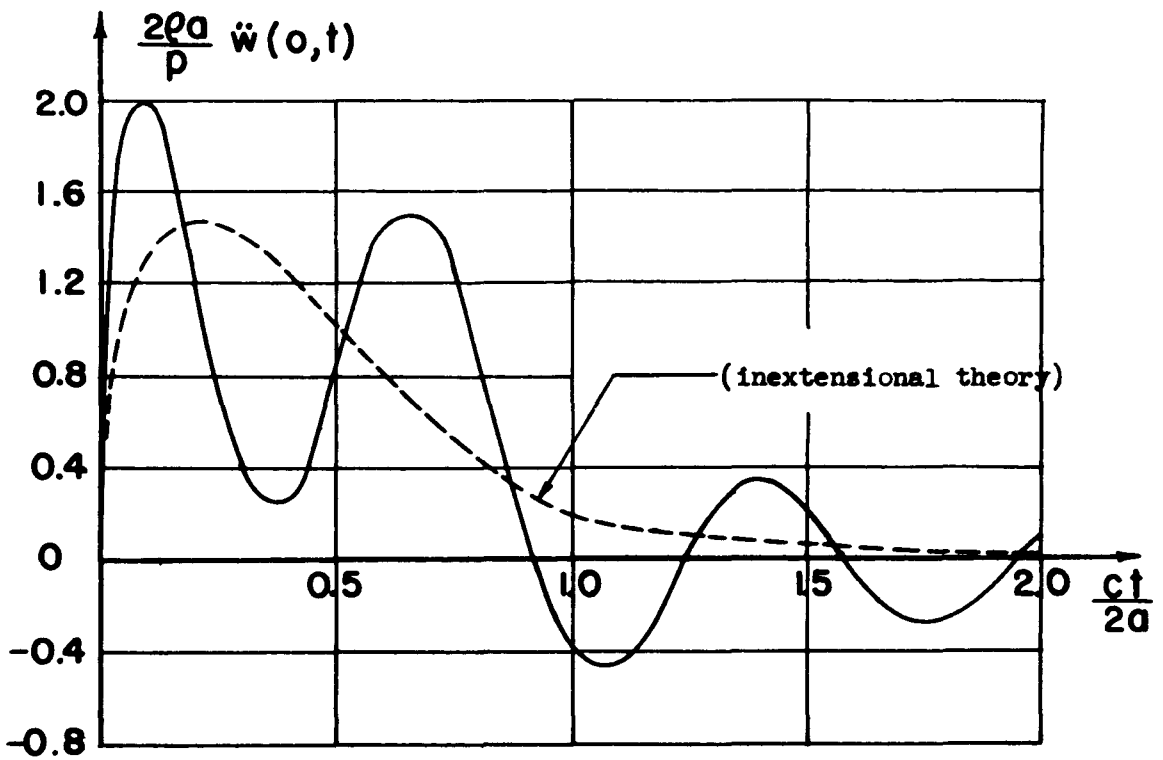

Fig. 4 Acceleration $\ddot{w}$ at $\theta = 0$ (for $n = 1, \frac{\rho a}{2m} = 1$).

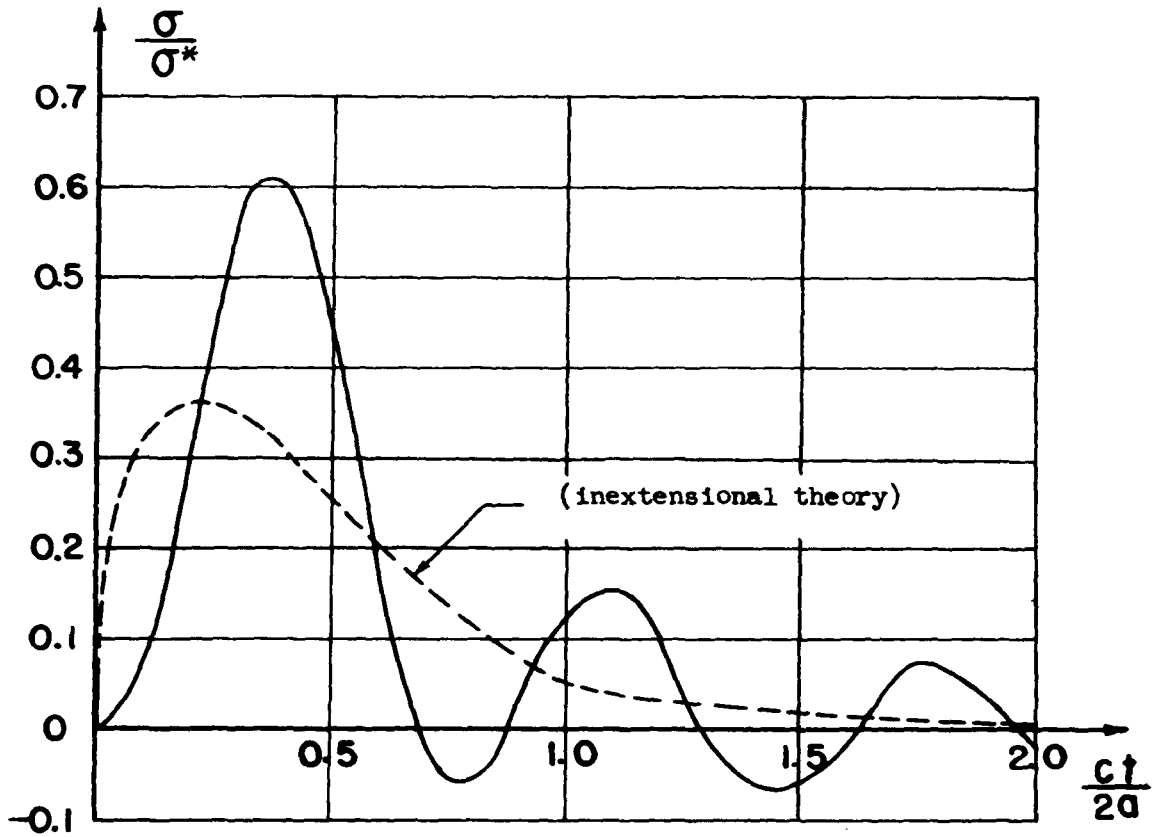

Fig. 5 Hoop Stress σ in Shell (for n = 1, $\frac{\rho a}{2m}$ = 1).

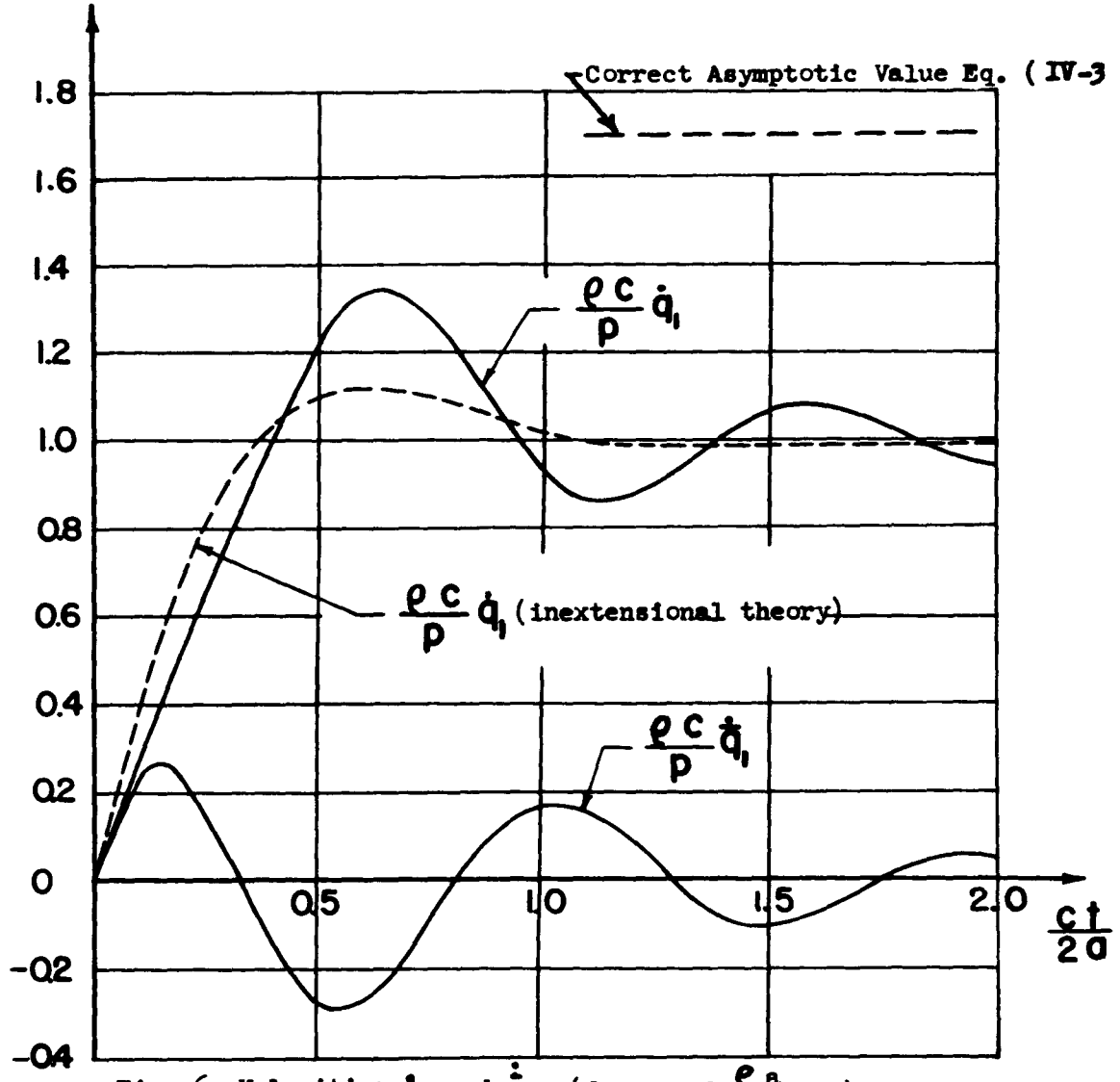

Fig. 6 Velocities $\dot{q}_1$ and $\dot{\dot{q}}_1$ (for $n = 1, \frac{\rho a}{2m} = 5$).

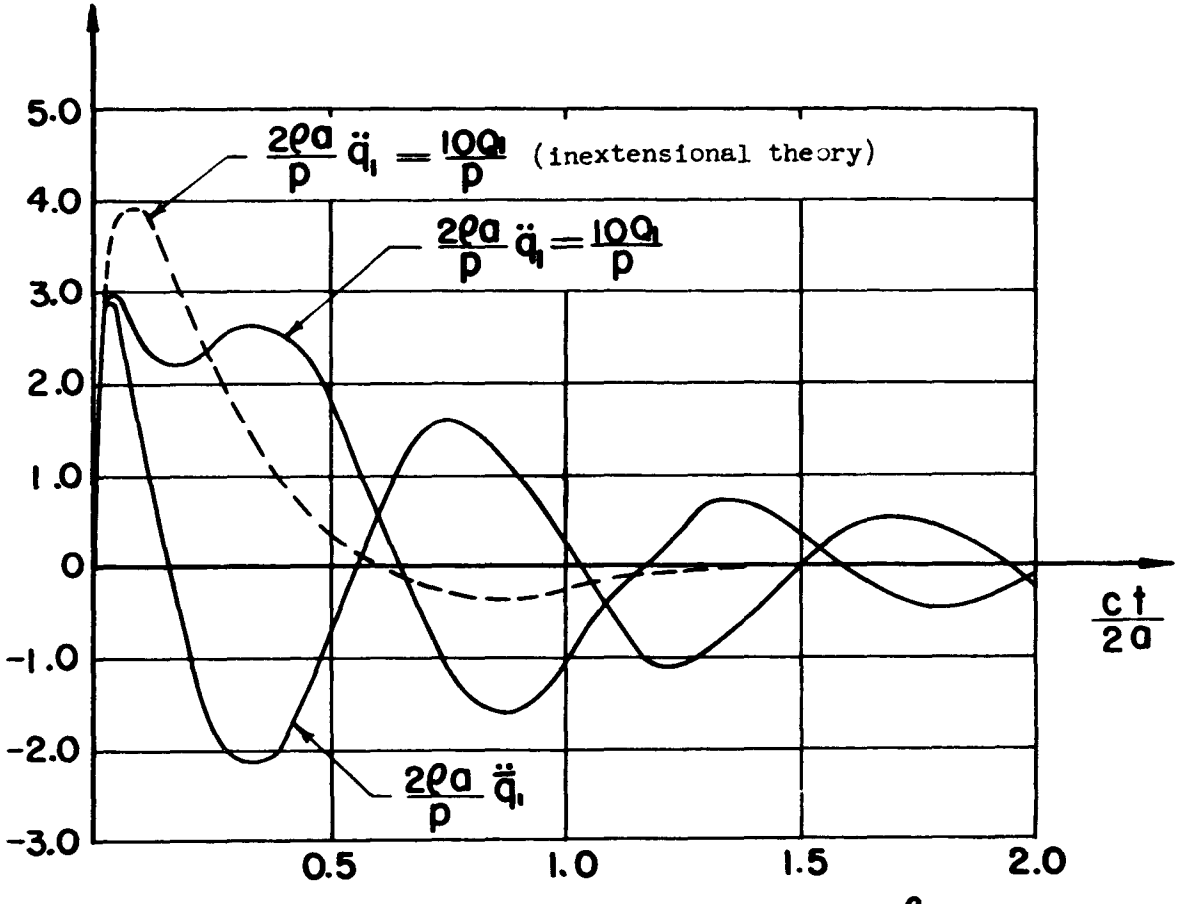

Fig. 7 Accelerations and Fluid Pressure (for n = 1, $\frac{\rho a}{2m} = 5$).

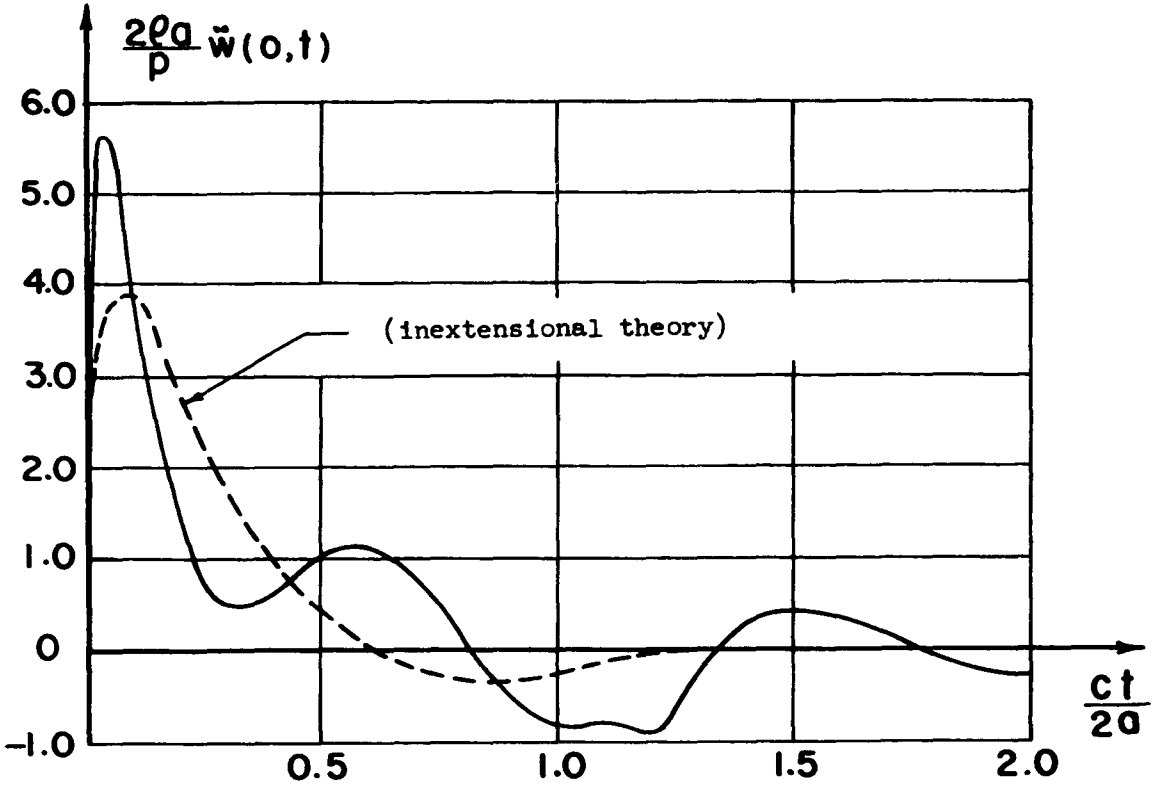

Fig. 8 Acceleration $\ddot{w}$ at $\theta = 0$ (for $n = 1, \frac{\rho a}{2m} = 5$).

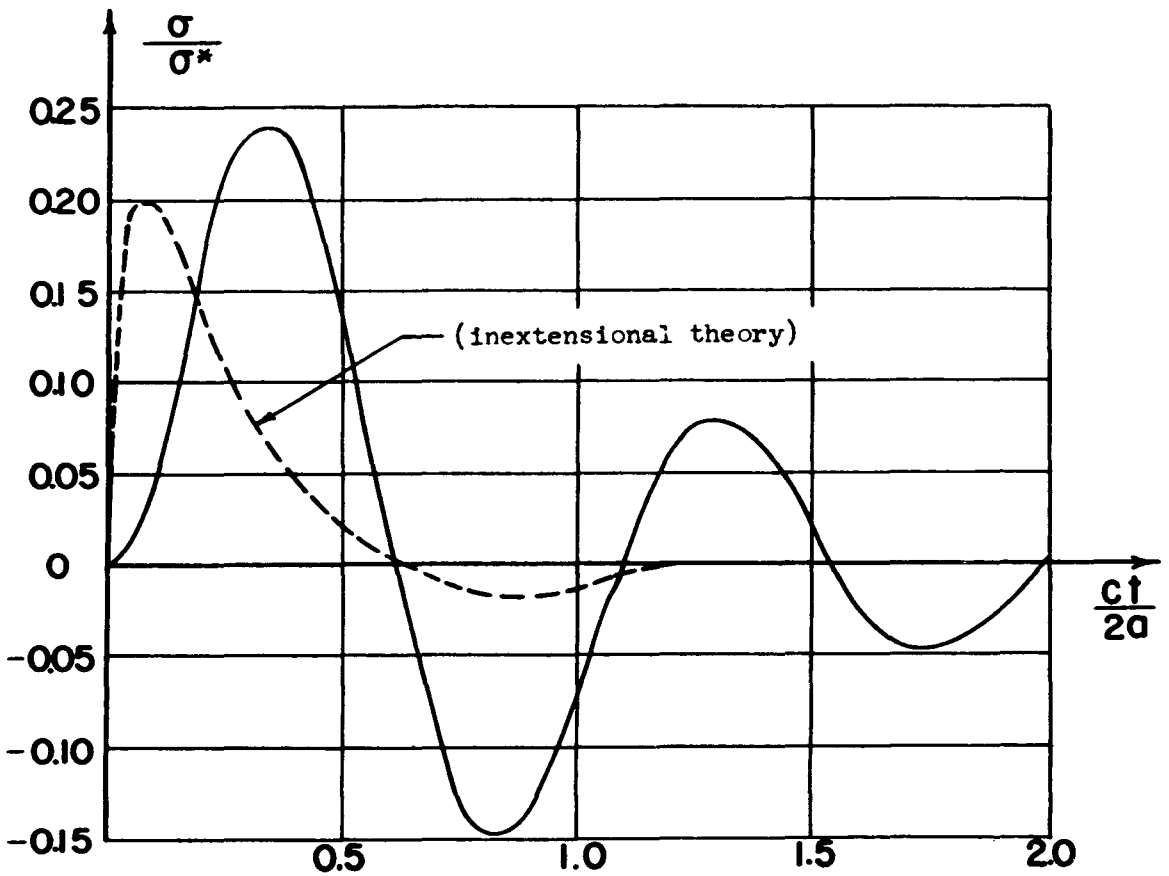

Fig. 9 Hoop Stress σ in Shell (for n = 1, $\frac{\rho a}{2m}$ = 5).

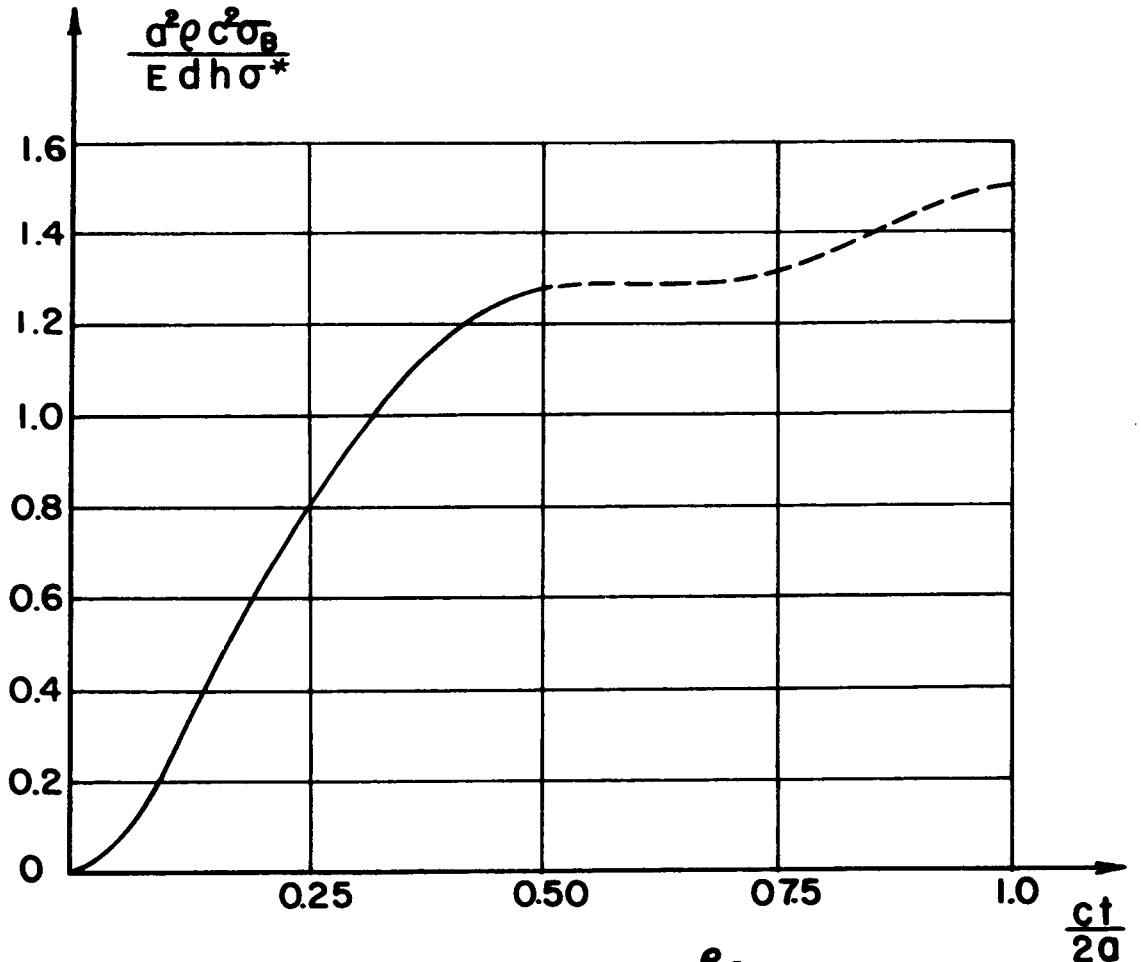

Fig. 10 Flexural Stress σ_B (for n = 2, $\frac{\rho a}{2m}$ = 5).

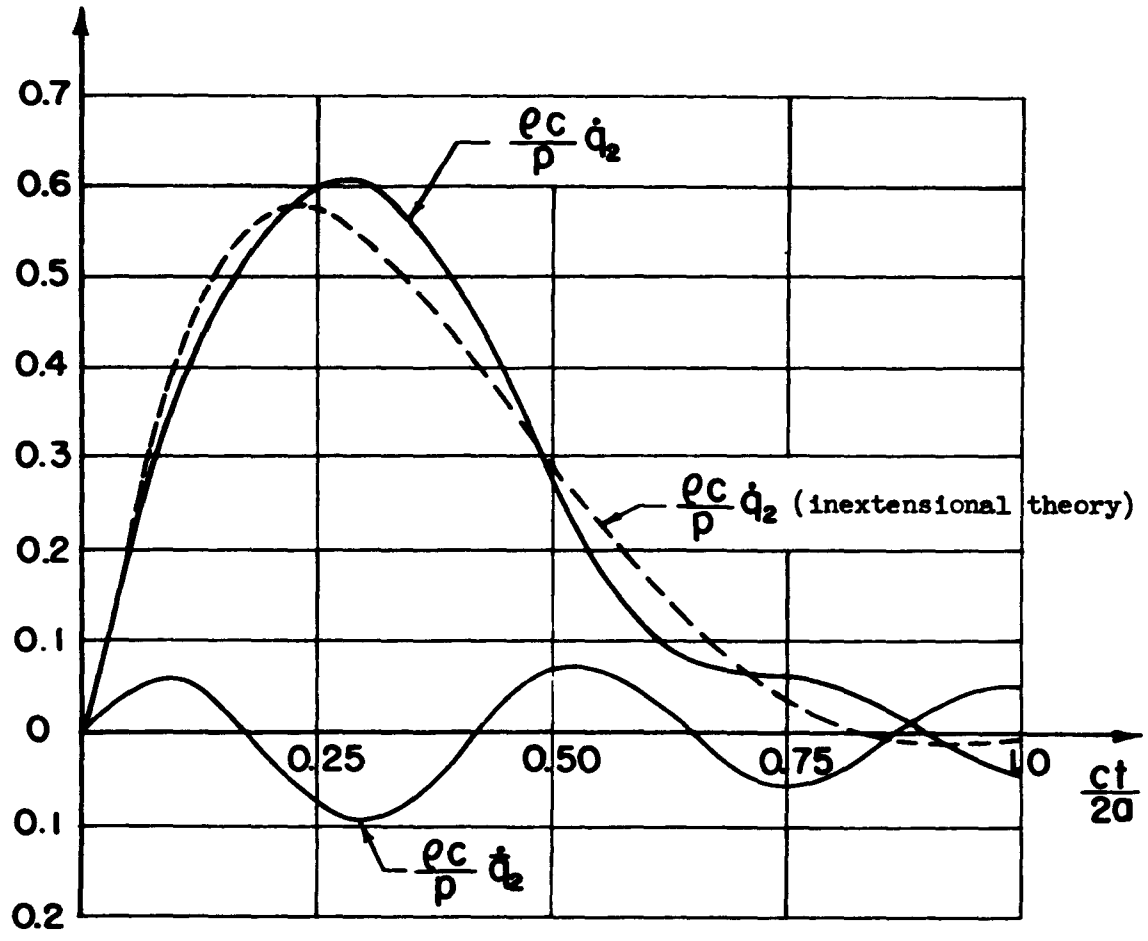

Fig. 11 Velocities $\dot{q}_2$ and $\dot{\bar{q}}_2$ (for $n = 2, \frac{\rho a}{2m} = 5$).

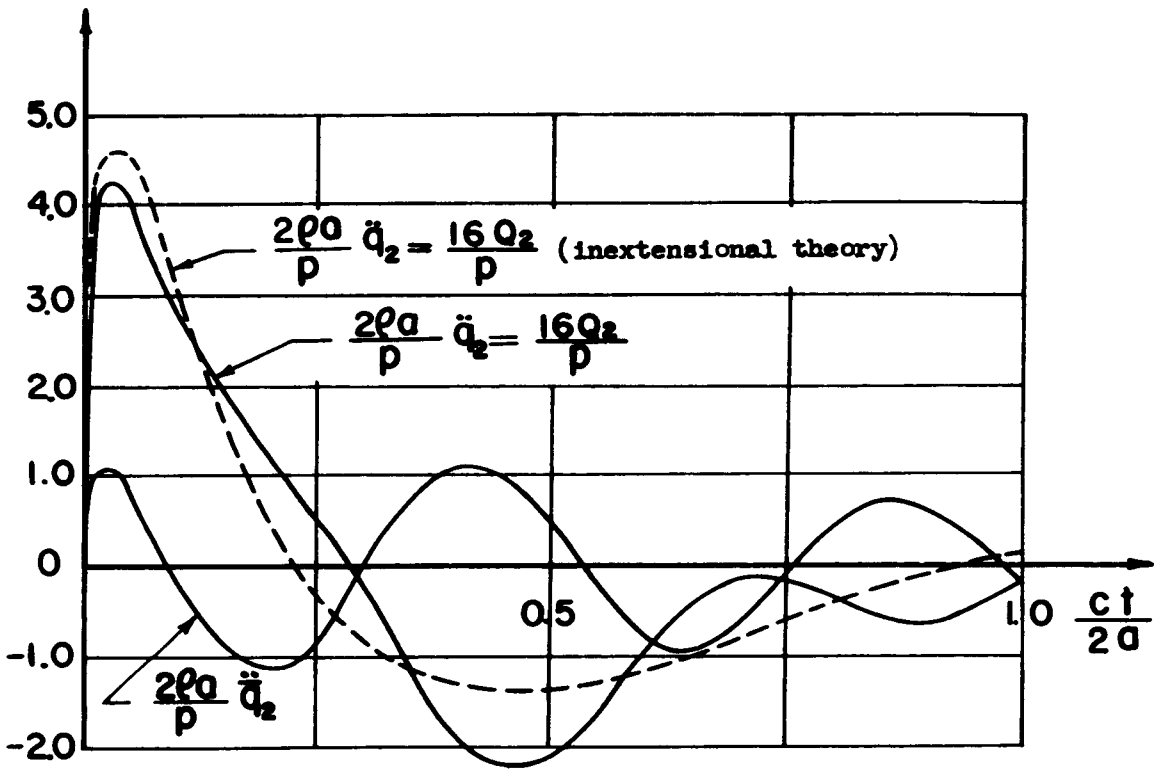

Fig. 12 Accelerations and Fluid Pressure (for n = 2, $\frac{\rho_s}{2\rho} = 5$).

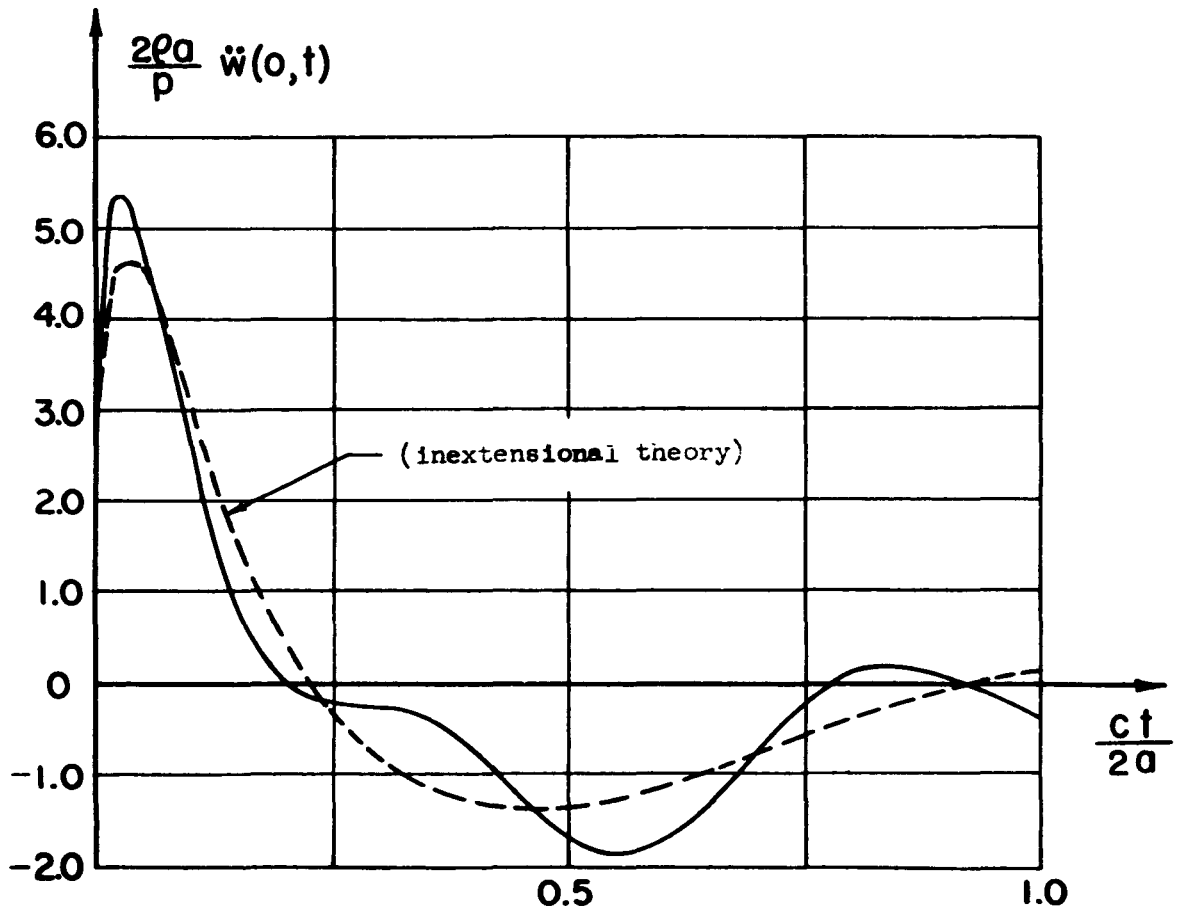

Fig. 13 Acceleration $\ddot{w}$ at $\theta = 0$ (for $n = 2, \frac{\rho a}{2m} = 5$).

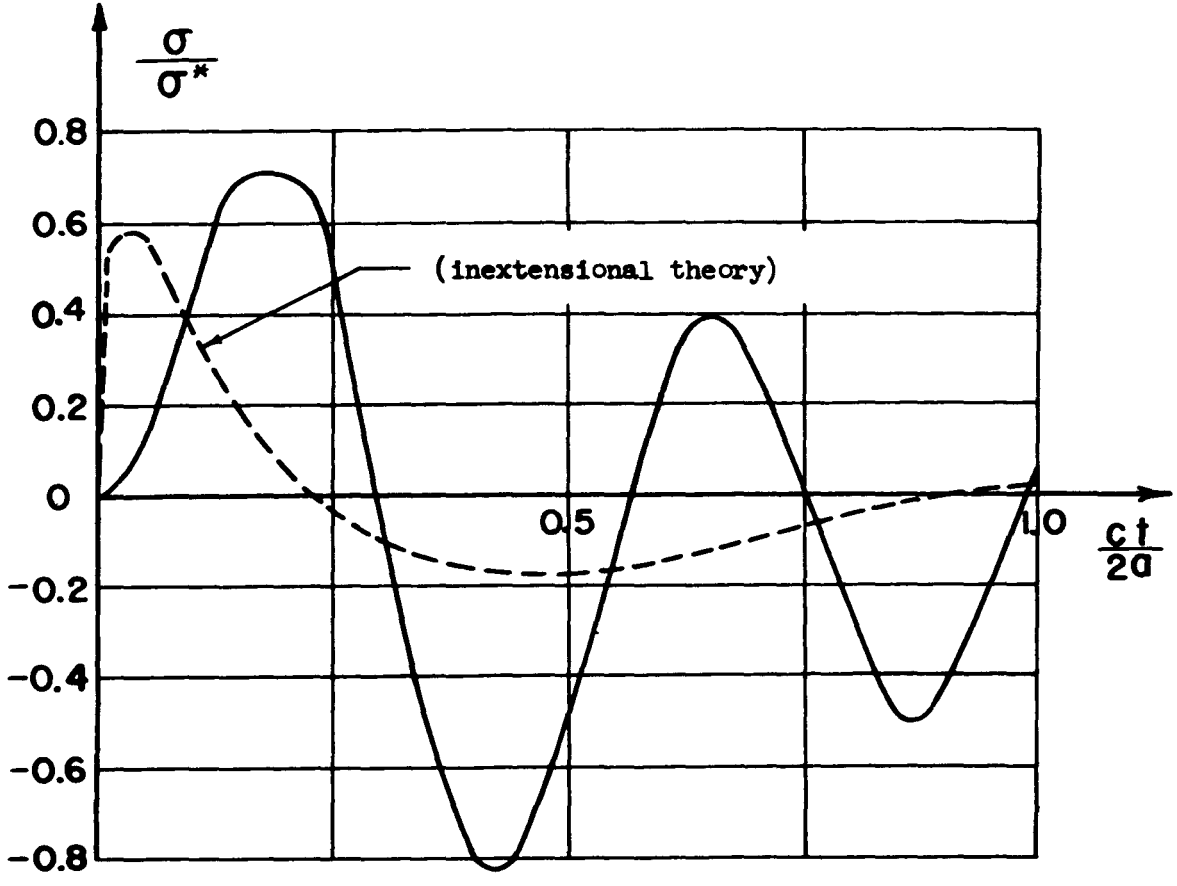

Fig. 14 Hoop Stress σ in Shell (for $n = 2, \frac{\rho a}{2m} = 5$).

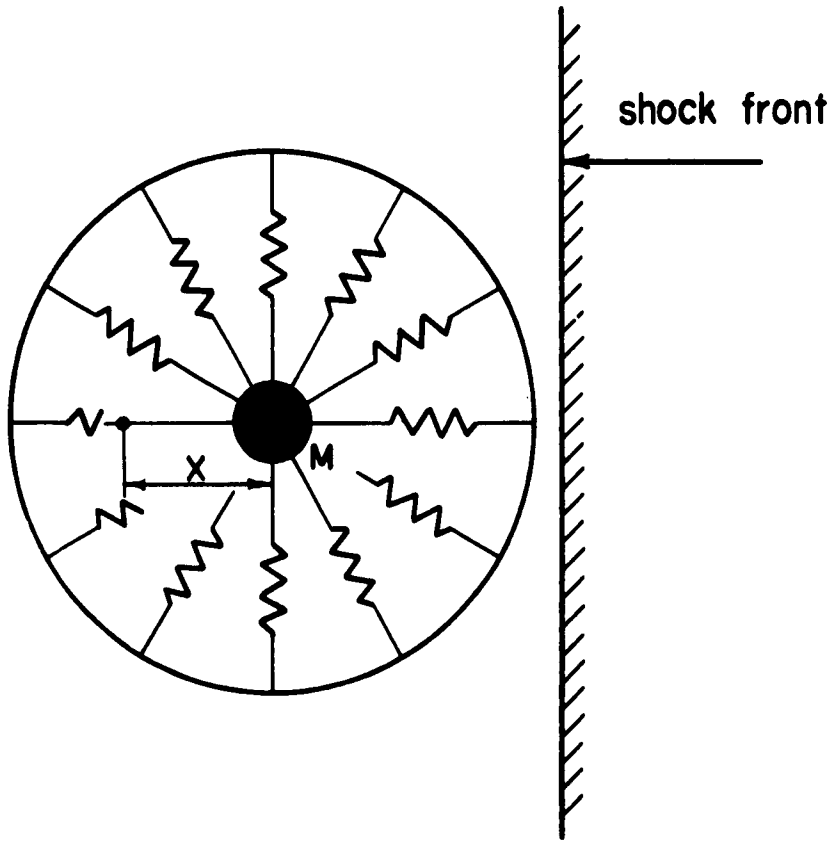

Figure 15

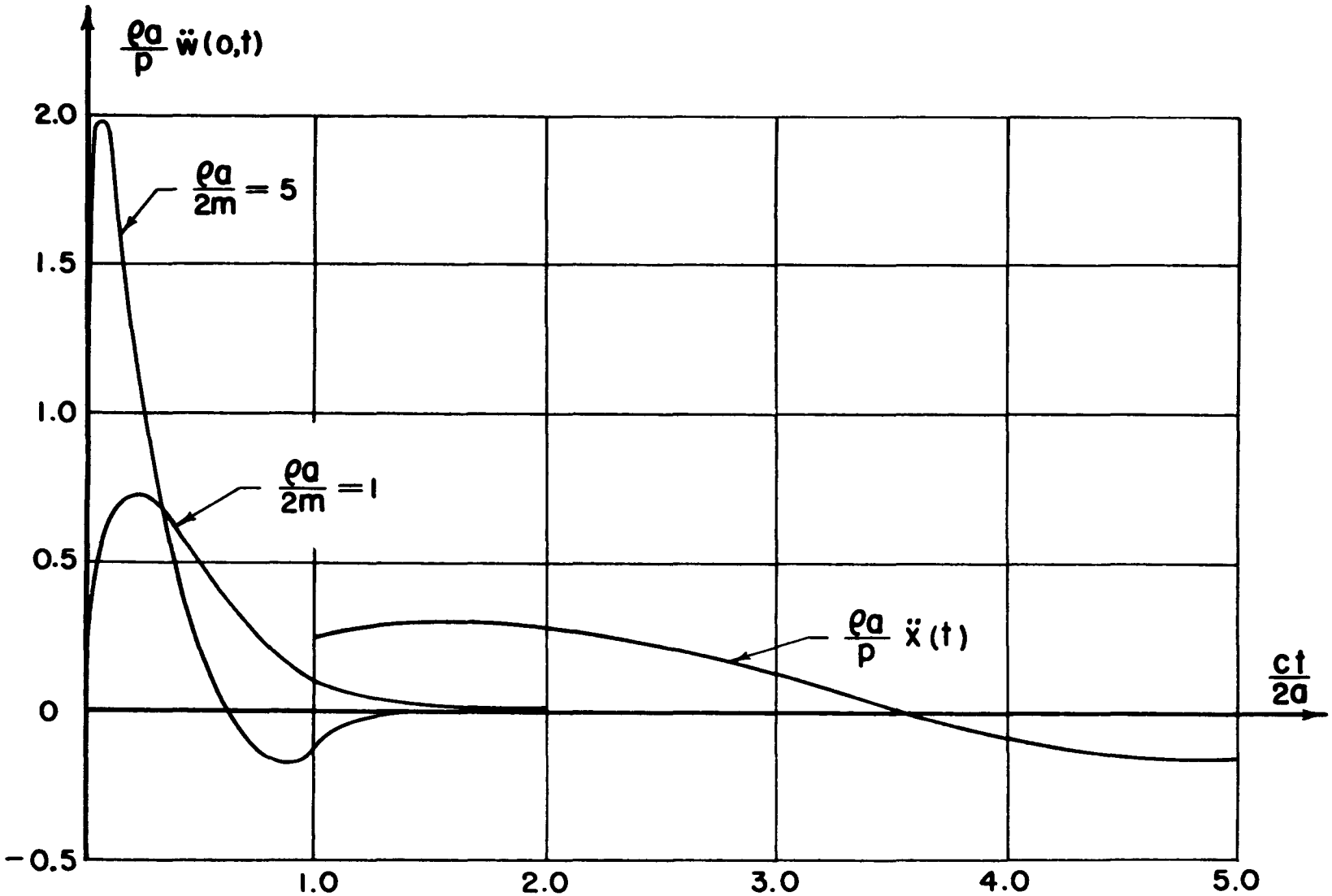

Fig.16 Acceleration $\ddot{x}$ of Mass at Center

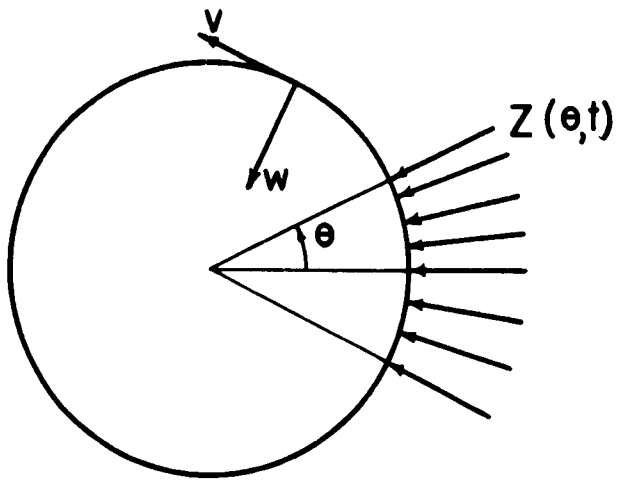

Figure 17

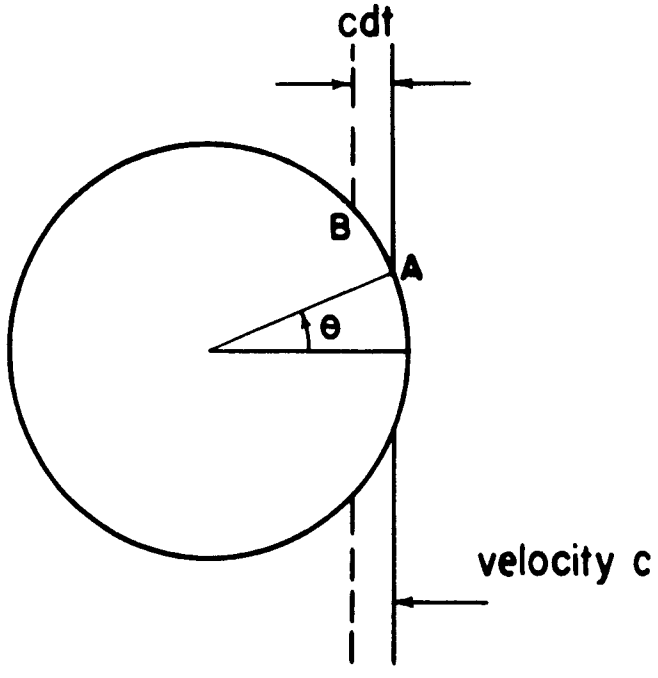

Figure 18

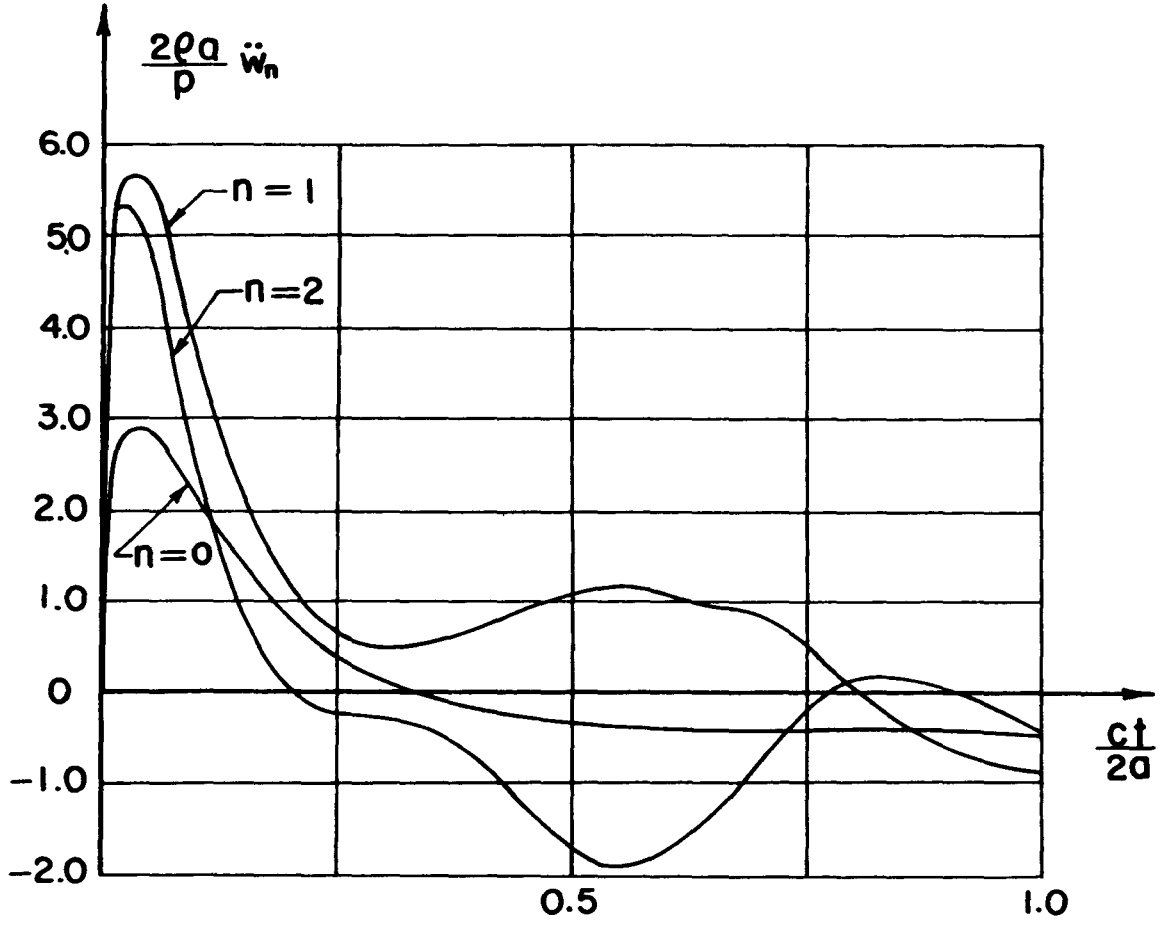

Fig. 19 Accelerations $\ddot{w}_n$ at $\theta = 0$ $(\frac{\rho a}{2m} = 5)$

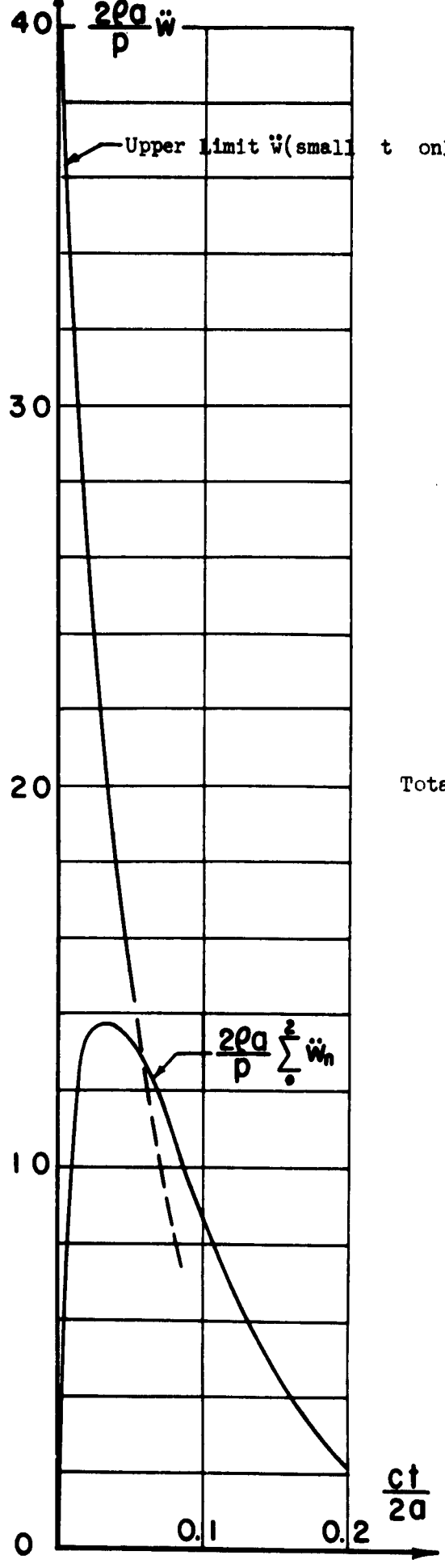

Figure 20

Total Acceleration $\ddot{w}(0,t)$

$(\frac{\rho a}{2m} = 5)$

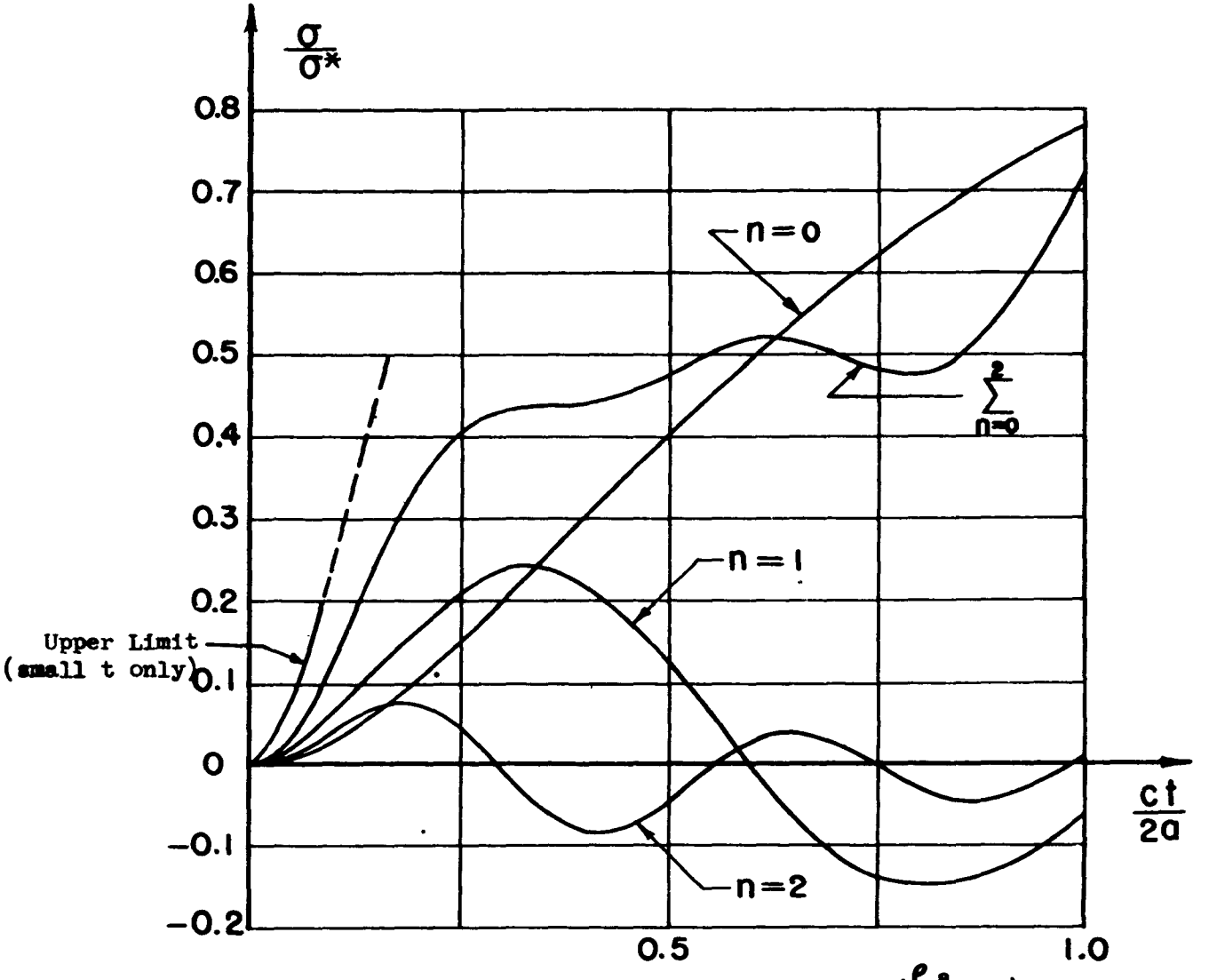

Fig. 21 Hoop Stress σ in Shell at $\theta = 0$ ($\frac{\rho a}{2m} = 5$)

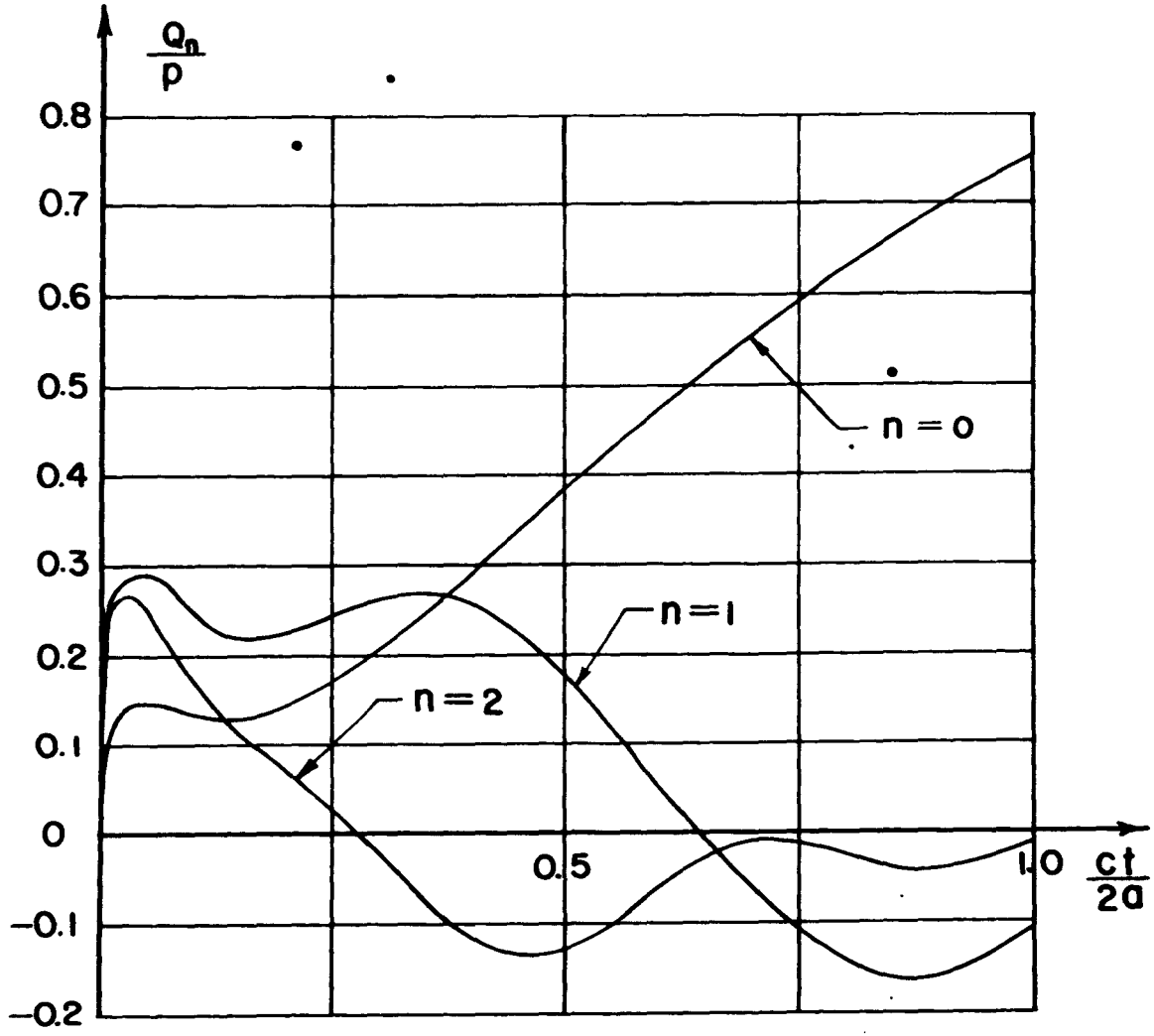

Fig. 22 Fluid Pressure on Shell ($\frac{\rho a}{2m} = 5$)

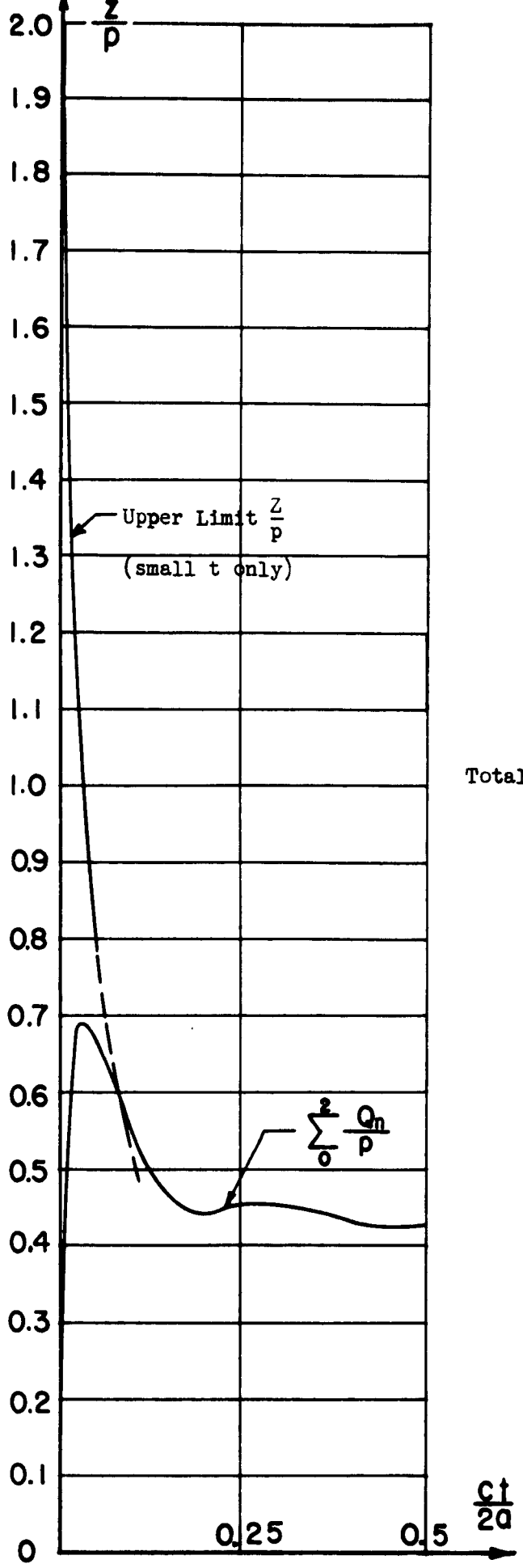

Figure 23

Total Fluid Pressure $Z(0,t)$

$(\frac{\rho a}{2m} = 5)$

Distribution List

for

Technical and Final Reports Issued Under

Office of Naval Research Project NR-360-002, Contract Nonr-266(08)

I: Administrative, Reference and Liaison Activities of ONR

Chief of Naval Research
Department of the Navy
Washington 25, D.C.
Attn: Code 438 (2)
Code 432 (1)
Code 466 (via Code 108) (1)

Director, Naval Research Lab.
Washington 25, D.C.
Attn: Tech. Info. Officer (9)
Technical Library (1)
Mechanics Division (2)

Commanding Officer
Office of Naval Research
Branch Office
346 Broadway
New York 13, New York (1)

Library of Congress
Washington 25, D.C.
Attn: Navy Research Section (2)

II: Department of Defense and Other Interested Government Activities

a) General

Research & Development Board
Department of Defense
Pentagon Building
Washington 25, D.C.
Attn: Library (Code 3D-1075) (1)

Armed Forces Special Weapons Project
P. O. Box 2610
Washington, D.C.
Attn: Lt. Col. G. F. Blunda (2)

British Joint Services Mission
Room 4906, Main Navy Building
18th and Constitution Avenue
Washington, D.C. (3)

b) Army

Chief of Staff
Department of the Army
Research & Development Division
Washington 25, D.C.
Attn: Chief of Res. & Dev. (1)

Engineer Res. & Dev. Lab.
Fort Belvoir, Virginia
Attn: Structures Branch (1)

The Commanding General
Field Command, AFSWP.
P. O. Box 5100, Albuquerque, N.M.
Attn: Col. Canterbury

Office of the Chief of Engineers
Assistant Chief for Works
Department of the Army
Bldg. T-7, Gravelly Point
Washington 25, D.C.
Attn: Structural Branch (R.L. Bloor) (1)

Office of the Chief of Engineers
Asst. Chief for Military Construction
Department of the Army
Bldg. T-3, Gravelly Point
Washington 25, D.C.
Attn: Structures Branch
(M. F. Carey) (1)
Protective Construction
Branch (I.O. Thornley) (1)

Army (cont.)

U.S. Army Waterways Experiment Sta.
P. O. Box 631
Halls Ferry Road
Vicksburg, Mississippi
Attn: Col. H. J. Skidmore (1)

Operations Research Officer
Department of the Army
Ft. Lesley J. McNair
Washington 25, D.C.
Attn: Howard Brackney (1)

c) Navy

Chief of Naval Operations
Department of the Navy
Washington 25, D.C.
Attn: OP-31 (1)
OP-363 (1)

Director, David Taylor Model Basin
Department of the Navy
Washington 7, D.C.
Attn: Code 720, Structures
Division (1)
Code 740, Hi-Speed
Dynamics Division (1)

Commander
Portsmouth Naval Shipyard
Portsmouth, N. H.
Attn: Design Division (1)

Naval Ordnance Laboratory
White Oak: Maryland
RFD 1, Silver Spring, Maryland
Attn: Mechanics Division (1)
Explosive Division (1)
Mech. Evaluation Div. (1)

Commander
U. S. Naval Ordnance Test Station
Inyokern, California
Post Office - China Lake, Calif.
Attn: Scientific Officer (1)

Chief of Bureau of Ships
Department of the Navy
Washington 25, D.C.
Attn: Code P-314 (1)
Code C-313 (1)

Superintendent
U.S. Naval Post Graduate School
Annapolis, Maryland

Ballistics Research Laboratory
Aberdeen Proving Ground
Aberdeen, Maryland
Attn: Dr. C. W. Lampson (1)

Office of Chief of Ordnance
Office of Ordnance Research
Department of the Army
The Pentagon Annex #2
Washington 25, D.C.
Attn: ORDTB-PS (1)

Chief of Bureau of Ships
Department of the Navy
Washington 25, D.C.
Attn: Director of Research (2)
Code 423 (1)
Code 442 (1)
Code 421 (1)

Officer in Charge
Underwater Explosions Research Div.
Code 290
Norfolk Naval Shipyard
Portsmouth, Virginia (1)

Director, Materials Laboratory
New York Naval Shipyard
Brooklyn 1, New York (1)

Chief of Bureau of Ordnance
Department of the Navy
Washington 25, D.C.
Attn: Ad-3, Technical Library (1)
Rec. P. H. Girouard (1)

Naval Ordnance Test Station
Underwater Ordnance Division
Pasadena, California
Attn: Structures Division (1)

Chief of Bureau of Aeronautics
Department of the Navy
Washington 25, D.C.
Attn: TD-41, Technical Library (1)

Officer in Charge
Naval Civil Engr. Research &
Evaluation Laboratory
Naval Station
Port Hueneme, California (1)

Commanding Officer & Director
U. S. Navy Electronics Lab.
San Diego 52, California
attn: Dr. A. B. Focke (1)

d) Air Forces

Commanding General
U. S. Air Forces
The Pentagon
Washington 25, D. C.
Attn: Res. & Development Div. (1)

Deputy Chief of Staff, Operations
Air Targets Division
Headquarters, U. S. Air Forces
Washington 25, D. C.
Attn: AFOIN-T/PV (1)

Office of Air Research
Wright-Patterson Air Force Base
Dayton, Ohio
Attn: Chief, Applied Mechanics Group (1)

e) Other Government Agencies

U. S. Atomic Energy Commission
Division of Research
Washington, D.C. (1)

Director, National Bur. of Standards
Washington, D.C.
Attn: Dr. W. H. Ramberg (1)

Supplementary Distribution List

Addressee	No. of Copies	
	Unclassified Reports	Classified Reports
Professor Lynn Beedle Fritz Engineering Laboratory Lehigh University Bethlehem, Pennsylvania	1	-
Professor R. L. Bisplinghoff Dept. of Aeronautical Engineering Massachusetts Institute of Technology Cambridge 39, Massachusetts	1	1
Professor Hans Bleich Dept. of Civil Engineering Columbia University Broadway at 117th St. New York 27, N. Y.	1	1
Professor B. A. Boley Dept. of Civil Engineering Columbia University Broadway at 117th St. New York 27, N.Y.	1	-
Professor G. F. Carrier Graduate Division of Applied Mathematics Brown University Providence, R.I.	1	-
Professor R. J. Dolan Dept. of Theoretical & Applied Mechanics University of Illinois Urbana, Illinois	1	-
Professor Lloyd Donnell Department of Mechanics Illinois Institute of Technology Technology Center Chicago 16, Illinois	1	-

Addressee	Unclassified Reports	Classified Reports
Professor A. C. Eringen Illinois Institute of Technology Department of Mechanics Technology Center Chicago 16, Illinois	1	-
Professor B. Fried Dept. of Mechanical Engineering Washington State College Pullman, Washington	1	-
Mr. Martin Goland Midwest Research Institute 4049 Pennsylvania Avenue Kansas City 2, Missouri	1	-
Dr. J. N. Goodier School of Engineering Stanford University Stanford, California	1	-
Professor R. M. Hermes College of Engineering University of Santa Clara Santa Clara, California	1	1
Professor R. J. Hansen Dept. of Civil & Sanitary Engineering Massachusetts Institute of Technology Cambridge 39, Massachusetts	1	-
Professor M. Hetenyi Walter P. Murphy Professor Northwestern University Evanston, Illinois	1	-
Dr. N. J. Hoff, Head Department of Aeronautical Engineering & Applied Mechanics Polytechnic Institute of Brooklyn 99 Livingston Street Brooklyn 2, New York	1	1
Dr. J. H. Hollomon General Electric Research Laboratories 1 River Road Schenectady, New York		
Dr. W. H. Hoppmann Department of Applied Mechanics Johns Hopkins University Baltimore, Maryland	1	-
Professor L. S. Jacobsen Department of Mechanical Engineering Stanford University Stanford, California	1	1

Addressee	Unclassified Reports	Classified Reports
Professor J. Kempner Department of Aeronautical Engineering and Applied Mechanics Polytechnic Institute of Brooklyn 99 Livingston Street Brooklyn 2, New York	1	-
Professor George Lee Department of Aeronautical Engineering Renssalaer Polytechnic Institute Troy, New York	1	-
Professor Paul Lieber Department of Aeronautical Engineering Renssalaer Polytechnic Institute Troy, New York	1	-
Professor Glen Murphy, Head Department of Theoretical & Applied Mechanics Iowa State College Ames, Iowa	1	-
Professor N. M. Newmark Department of Civil Engineering University of Illinois Urbana, Illinois	1	1
Professor Jesse Ormondroyd University of Michigan Ann Arbor, Michigan	1	-
George B. Peagram Chairman, Committee on Government Aided Research Columbia University, New York, 27, N. Y.	1	-
Dr. R. P. Petersen, Director Applied Physics Division Sandia Laboratory Albuquerque, New Mexico	1	1
Dr. A. Phillips School of Engineering Stanford University Stanford, California	1	-
Dr. W. Prager, Chairman Graduate Division of Applied Mathematics Brown University Providence 12, R.I.	1	1
Dr. S. Raynor Armour Research Foundation Illinois Institute of Technology Chicago, Illinois	1	-

Addressee	Unclassified Reports	Classified Reports
Professor E. Reissner Department of Mathematics Massachusetts Institute of Technology Cambridge 39, Massachusetts	1	-
Professor M. A. Sadowsky Illinois Institute of Technology Technology Center Chicago 16, Illinois	1	-
Professor M. G. Salvadori Department of Civil Engineering Columbia University Broadway at 117th Street New York 27, New York	1	-
Professor J. E. Stallmeyer Talbot Laboratory Department of Civil Engineering University of Illinois Urbana, Illinois	1	1
Professor E. Sternberg Illinois Institute of Technology Technology Center Chicago 16, Illinois	1	-
Professor F. K. Teichmann Department of Aeronautical Engineering New York University University Heights, Bronx New York, N. Y.	1	-
Professor C. T. Wang Department of Aeronautical Engineering New York University University Heights, Bronx New York, N. Y.	1	-
Project File	2	2
Project Staff	5	-
For possible future distribution by the University	10	-
To ONR Code 438, for possible future distribution	-	10